https://doi.org/10.1016/j.jeurceramsoc.2021.11.019

Design, fabrication and properties of lightweight wear lining refractories: A review

Lvping Fu [1,2] *, Huazhi Gu [1] *, Ao Huang [1], Siu Wing Or [2] *, Yang Zou [1], Yongshun Zou [1], Meijie Zhang [1]

[1] The State Key Laboratory of Refractories and Metallurgy, Wuhan University of Science and Technology, Wuhan 430081, China

[2] Department of Electrical Engineering, The Hong Kong Polytechnic University, Hung Hom, Kowloon, Hong Kong, China

*Corresponding author

Abstract

The design of lightweight wear linings is crucial in terms of the energy and resource efficiency of industrial furnaces and quality of final products. This review aims to present a systematic overview of the design, fabrication, properties, and application of lightweight wear lining refractories. The crucial properties and process routes of lightweight aggregates are summarised. Then, the structural design and factors that affect the refractories are described, and the application efficiency of the refractories is evaluated. Further, the scope for future work on this topic is presented.

Key words: Energy saving; lightweight; wear lining; refractories; thermal conductivity

1 Introduction

High-temperature industries are the basic industries for the production of both structural materials (iron & steel, glasses, ceramics, etc.) and advanced functional materials (sensors, absorbing materials, catalysts, energy storages materials, etc.). Refractory linings, which are fundamental in high-temperature industrial furnaces, play a crucial role in the efficiency and quality of high-temperature industries. On the one hand, compared to radiation and exhaust gases, heat dissipation through linings is the principal heat loss route employed in industrial furnaces [1,2]. The heat insulation performance of refractory linings is among the primary factors that decide the energy efficiency and consumption of high-temperature furnaces [3]. On the other hand, refractory linings are involved in the entire high-temperature production process; hence, they lead to undesirable inclusions in the final products (i.e. steel, iron, alloy, glass) [4-6]. To improve the quality and cleanliness of the products, developing long-lasting refractory linings is a prerequisite. Therefore, designing long-lasting and energy-saving refractory linings is essential for high-temperature industrial processes.

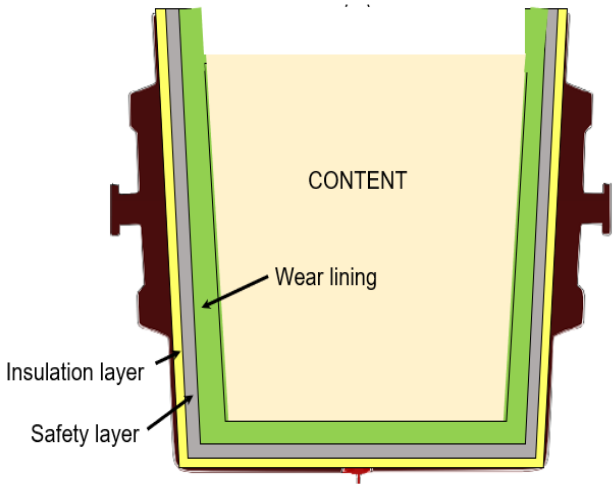

Fig. 1. Conventional structure of a high-temperature industrial furnace. It typically possesses a multi-layer lining, consisting of layers of different thickness and made of materials with different performances.

As shown in Fig. 1, a conventional refractory lining structure has a wear lining, safety layer, and an insulation layer. The wear lining resists erosion, wear, corrosion and thermomechanical loads of molten melts, while the insulation layer reduces the thermal transfer through refractory lining. Several studies investigated methods to extend the life span of wear linings and reduce the thermal conductivity of the insulation layer. This led to significant advances in the high-temperature industrial furnaces, while the following two issues emerged.

(i) To improve the resistance to chemical corrosion, abrasion, and thermal spalling of wear linings, researchers have attempted to enhance the purity, density, and strength of aggregate materials. Although this resulted in a longer life span of wear linings, it also lead to property mismatching between the aggregates and matrices in the refractory materials. Owing to a higher porosity of a matrix than that of the aggregates, the damage and degradation would preferentially occur at the matrix of the refractories. The analysis of used wear lining refractories showed that most aggregates were just slightly damaged, indicating excessively high density of the aggregates [7-9].

(ii) For the insulation layer, a series of novel thermal insulation materials have been developed. Among them, nano-insulation boards, which show a lower thermal conductivity than air, have been predominantly studied [10]. Conventionally, the maximum use temperature of nano-insulation board is below 1000 °C. However, for most steel-making industrial furnaces, the temperature at the interface between the safety and insultation layers is 1000−1200 °C. The pulverisation, degradation, and failure of a nano-insulation board occur only after 3−5 heating cycles; consequently, the thermal insulation performance of the linings is degraded [11].

To overcome the above-mentioned two problems, the idea of designing a lightweight

wear lining refractory containing lightweight aggregates has been proposed by researchers at the beginning of the present century. On the one hand, as mentioned above, because the matrix is the weaker part during the service process of refractories, aggregates with excessively high density are not usually necessary. Energy and resource consumption could be reduced by replacing conventional dense aggregates with lightweight porous aggregates. On the other hand, the thermal conductivity of wear linings could be decreased by employing lightweight porous aggregates. Further, the temperature field distribution of refractory linings can be optimised and interface temperature between the safety and insultation layers can be reduced to an acceptable value for a nano-insulation board. Therefore, the heat dissipation through linings could be significantly decreased. And more importantly, the superheat degree of molten melts could be decreased [12], leading to improved quality of final products. In 2003, a lightweight wear lining refractory was first reported by Chen et al., who fabricated a low-density spinel-alumina ladle castable using porous alumina as aggregates [13]. Later, a series of lightweight porous aggregates (alumina, mullite, spinel, and cordierite) was prepared via an in-situ pore-forming technique by Li et al. [14] and Yan et al. [15-19]. In addition, lightweight porous aggregates of calcium aluminates and spinel have been reported [20,21]. Compared to common dense refractory materials, the lightweight refractories fabricated with such lightweight aggregates exhibited lower bulk density and thermal conductivity [19,21]. However, the key challenge is the slag attack resistance and mechanical properties of materials [19,22,23].

To obtain lightweight refractories with guaranteed resistance to slag corrosion and stress failure, numerous attempts have been conducted to fabricate lightweight aggregates with a high proportion of closed pores and small pore size. The superplastic foaming method was proposed by Kishimoto et al. to fabricate ceramics with a high volume fraction of fine closed

pores [24,25]. Lightweight micro-pored alumina, bauxite, and magnesia materials obtained by adding nano-additives have been reported by Gu et al. and Fu et al.; in these materials, the proportion of closed pores was approximately 40−70% of the total pores [26-30]. Furthermore, owing to reductions in pore size, the fabricated lightweight materials could show improved slag corrosion resistance compared to dense materials [31-33]. Besides the fabrication of lightweight aggregates, several studies focused on the matrix particle packing and service conditions of lightweight wear lining refractories [34,35]. Additionally, a novel lightweight refractory with a density gradient was prepared in recent years [36,37].

Consequently, this review focuses on the systematic elucidation of the design, fabrication, and application of lightweight wear lining refractories. First, the crucial properties and process routes of the lightweight aggregates are presented and summarised. Then, the design and fabrication of lightweight wear lining refractories are described, and the factors that affect the properties of the fabricated lightweight refractories are discussed. Finally, the challenges faced and scope for future work in this field are presented.

2. Lightweight aggregates

Besides the route of carbothermal reduction of MgO proposed by Yin et al. [37], all the reported lightweight refractories are produced by replacing dense aggregates with lightweight aggregates. Therefore, the performance of lightweight refractories is dependent on the structure and properties of lightweight aggregates. In the following section, the parameters of the porous structure that affect the properties of lightweight aggregates are discussed. Then, the processing methods required for the fabrication of lightweight aggregates and data on their properties, available in the literature, are summarised.

2.1 Crucial properties

2.1.1 Parameters of porosity structure

The pore structure parameters (porosity, size distribution, and location) are the key factors that affect the properties of the lightweight aggregates. As shown in Fig. 2 (a), based on the pore interconnectivity, the porosity in lightweight aggregates is divided into two categories: open porosity and closed porosity. Open porosity refers to the pores which are interconnected to the outside environment, while closed porosity corresponds to the pores that are isolated from the environment. Based on their location, pores are classified as intercrystalline or intracrystalline; the former is located on grain boundaries (Fig. 2 (c)), while the latter is trapped inside the grains (Fig. 2 (b)).

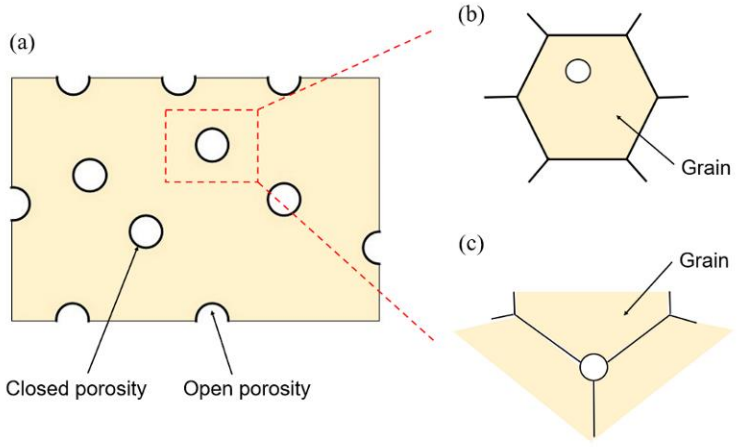

Fig. 2. Porosity structure in lightweight aggregates. Based on the interconnectivity and location of pores, they could be classified as open or closed porosity (shown in (a)) and intracrystalline or intercrystalline pores (presented in (b) and (c)).

For a lightweight aggregate with a fixed total porosity, the crucial properties (heat insulation, strength, and slag attack resistance) could be improved by decreasing the pore size and increasing the proportion of closed and intracrystalline pores. For lightweight aggregates fabricated via different methods, the pore size could be influenced by the particle size of raw materials, type and size of pore-forming agent, heat treatment, and additives [38-40].

The lightweight aggregates are typically produced from ceramic powders, thus, the

microstructural evolution of lightweight aggregates during sintering is very similar to that of ceramic materials. During the sintering and densification process of powders, the migration of pores and grain boundaries are the two main factors that affect the formation of closed and intracrystalline pores [41]. Generally, during the sintering process, the migration rate of pores is greater than that of grain boundaries, indicating that the pores restrict the movement of grain boundaries [41-43]. In this case, the pores are eliminated or left in the sample as open pores (Fig. 3 (a)). Contrarily, if the migration speed of grain boundaries is greater than that of pores, the grain boundaries can move freely without the restriction of the pores. In this case, the separation of pores from the grain boundaries occurs, and the pores are closed by the grain boundaries before being eliminated [41-43]. This eventually leads to the formation of intracrystalline pores (Fig. 3 (b)).

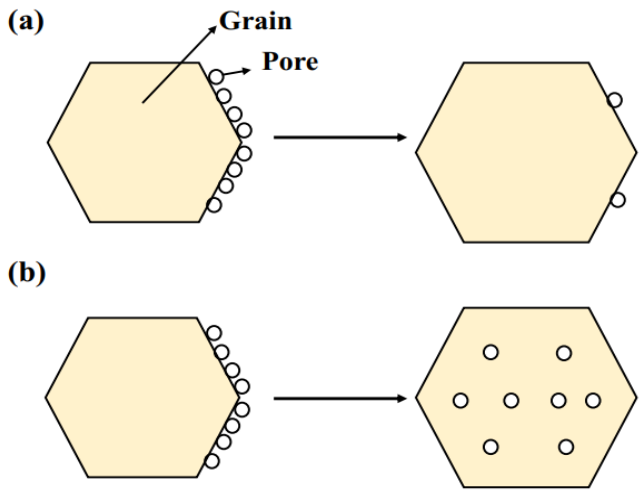

Fig. 3. Migration of grain boundaries and pores during the sintering process. Open pores would be produced when the migration rate of pores is greater than that of grain boundaries (shown in (a)). Otherwise, pores would be trapped in grains and transformed to intracrystalline pores (presented in (b)).

2.1.2 Heat insulation

Heat transport through a lightweight aggregate considered as a solid−gaseous material

with two phases mainly involves heat conduction due to the solid and gas phases, and heat convection and radiation through pores. The heat conduction is directly proportional to the porosity of the materials. Because gas phases typically possess lower thermal conductivity than solid phases, increasing porosity would result in lower heat conduction [44,45]. In addition, decreased pore size would also lead to lower heat conduction [46-48]. That is because with the reduction in pore size, the number of gas-solid interfaces would be increased, resulting in longer heat conduction distance along the solid phase and greater heat resistance. Moreover, the pore size has a significant influence on the heat convection and radiation. A decreased pore size results in lower heat convection and radiation. The contribution of heat convection and radiation to the equivalent thermal conductivity of thermal lightweight aggregates increases with increasing temperature. Several models have been proposed to predict the thermal conductivity of porous ceramics [49-51]. A modified exponential relation has been established by Živcová et al. to describe the porosity dependence of the effective thermal conductivity of porous alumina [50]. Pia et al. proposed an intermingled fractal unit model to evaluate the influence of pore shape on the thermal conductivity of porous ceramics [49,51]. The equivalent thermal conductivity of a lightweight aggregate at a low temperature is mainly affected by porosity, while the influence of pore size is significant at high temperatures [52,53].

Besides the porosity and pore size, the distribution of pores results in differences in the equivalent thermal conductivity of lightweight aggregates. The effect of pore distribution on the equivalent thermal conductivities of porous materials was investigated [54,55]. As shown in Fig. 4, for a fixed total porosity and average pore diameter, when the distribution of pore size and position is nonuniform, the direction of the heat flow line changes continuously. This results in higher heat resistance and lower effective thermal conductivity. Therefore, to

improve the heat insulation of lightweight refractories, lightweight aggregates with a multiscale pore size distribution are desired.

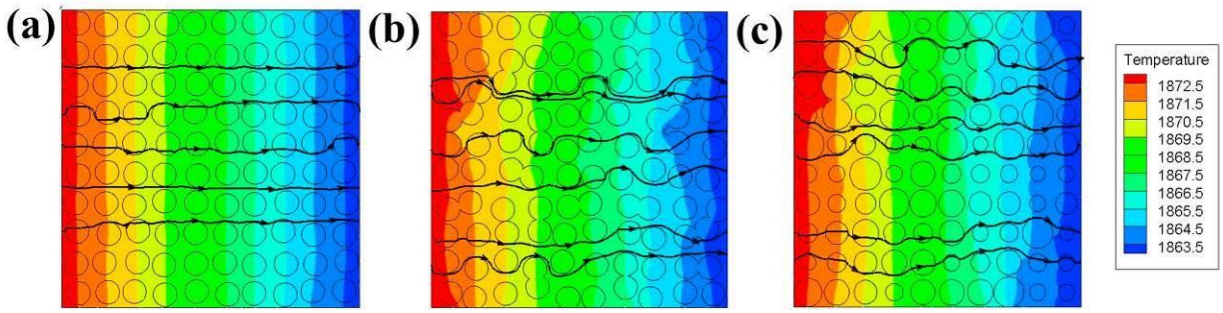

Fig. 4. Heat flow streamlines of porous material with (a) uniform pore distribution, (b) nonuniform distribution in pore position, and (c) nonuniform distribution in pore size. Heat flow lines are lengthened when the pores are non-uniformly distributed. Adapted from Ref. [54], Copyright (2018) with permission from Elsevier.

2.1.3 Slag attack resistance

Because the porosity of lightweight aggregates provides potential channels for slag penetration, the slag attack resistance of fabricated lightweight aggregates is a crucial property for the development of lightweight wear lining refractories. It is generally accepted that the slag resistance of lightweight aggregates can be improved by reducing the open porosity and pore size [56,57]. To further identify the correlation between pore structure characters and slag corrosion behaviours of lightweight refractories, slag corrosion of lightweight aggregates was investigated using simulation methods. As shown in Fig. 5, increasing the pore size and open porosity results in deeper slag penetration and corrosion. When compared to open porosity, the pore size of lightweight aggregates has a crucial impact on the slag penetration. An increase in

pore size results in significant degradation of slag resistance performance. This inference has also been confirmed by experimental results [32]. Therefore, to improve the slag resistance performance, more attention should be paid to the pore size during the fabrication of lightweight aggregates.

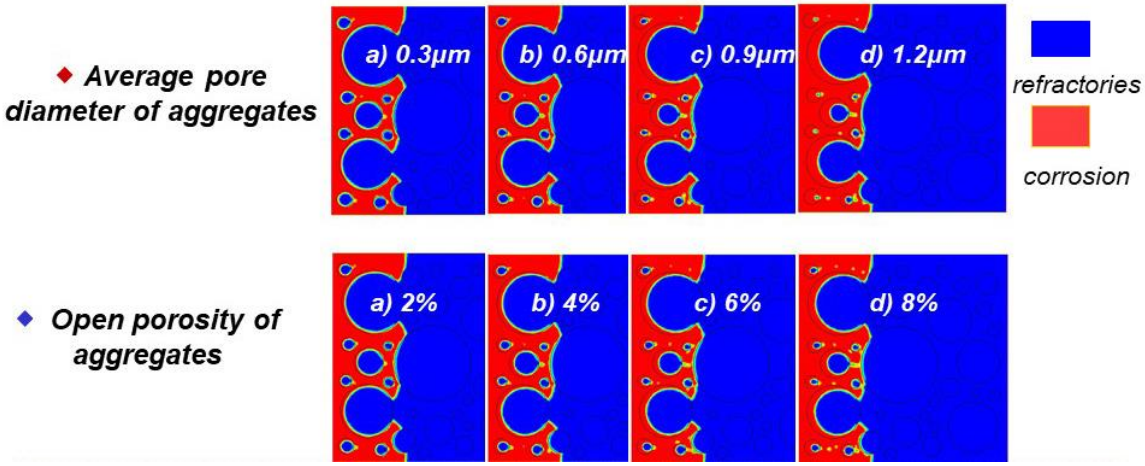

Fig. 5. Slag corrosion of lightweight refractories containing lightweight aggregates with different pore sizes and open porosities. Increasing open porosity or pore size of lightweight aggregates would increase the surface area exposed to the molten slag, resulting in deeper slag attack. The pore size has more significant impact on the slag attack resistance of lightweight refractories.

2.1.4 Mechanical and thermomechanical properties

To understand the influence of pores on the mechanical properties of brittle materials, Inglis proposed a model to calculate the stress concentration effect caused by ellipsoidal pores, as shown in Equation (1) [58].

$$(\sigma_{yy})_p = 2\sigma_a\left(\frac{R}{r}\right) \quad (1)$$

where $(\sigma_{yy})_p$ is the maximum tensile stress, σ_a is the applied tensile stress on the pore, and R and r are the long and short axes of the pore, respectively.

Generally, in most cases, the pores are approximately spherical, indicating the *R/r* value of pores in ceramic materials is relatively low. According to Equation (1), the stress concentration effect caused by the pores is not very significant.

Although a single pore can hardly be considered a crack in ceramic materials, the amount, size, distribution, and location of pores influence crack formation and propagation in brittle materials.

The effect of porosity on the fracture energy of ceramic materials was investigated by Vandeperre et al. [59]. As shown in Fig. 6, the fracture energy of alumina materials remains almost constant up to a pore volume fraction of 0.15−0.25. In this case, the required force for crack growth between two pores could be greater than that in a completely dense material. However, a porosity greater than 0.25 results in the crack−pore interaction, leading to a sharp degradation of mechanical properties. However, the pore size is another critical factor. The strengthening effect would be enhanced or weakened in different pore size level [60,61].

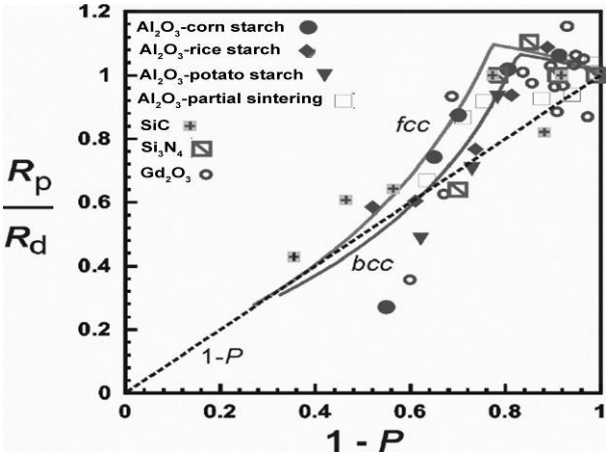

Fig. 6. Fracture energy normalized by the fracture energy of dense material. The abscissa is the relative density of materials, while the ordinate is the relative fracture energy.

Adapted from Ref. [59], Copyright (2004) with permission from Taylor & Francis.

In terms of the location of pores, when pores are located on grain boundaries, the

localized stress may overcome the bonding strength between grains and cause the looseness of boundaries, resulting in the fracture of materials. However, in the case of intracrystalline pores, as the bonding strength in the grains is high, the stress concentration might be alleviated.

Influence of pore structure on the thermomechanical behaviours of lightweight refractory materials was studied by Luo et al., who reported that highest thermal shock resistance is achieved when the porosity of materials is approximately 20% (as shown in Fig. 7). Moreover, a uniform distribution of pores is favourable in terms of the thermomechanical behaviours of lightweight refractories [62]. Thus, in brief, to obtain lightweight refractories with good mechanical and thermomechanical properties, the total porosity should be controlled around 20%.

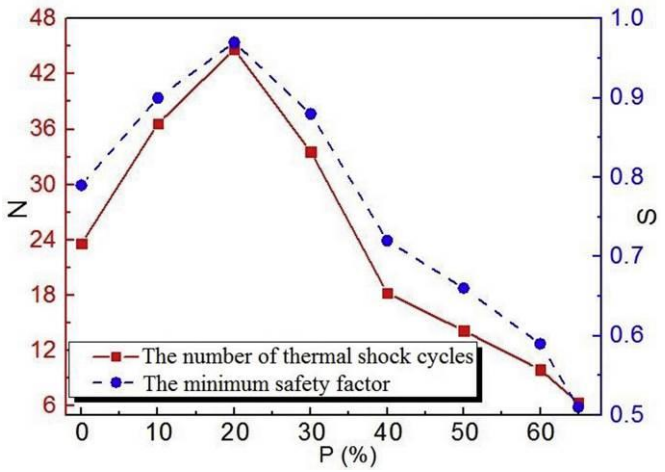

Fig. 7. The number of thermal shock cycles and minimum safety factor versus porosity. A higher thermal shock cycles number and minimum safety factor suggesting better thermal shock resistance performance.

Reprinted from Ref. [62], Copyright (2020) with permission from Elsevier.

2.2 Processing routes

In general, process routes for the fabrication of lightweight aggregates are adapted from

the processing of porous ceramics. However, for the preparation of lightweight aggregates, the cost and operating convenience for large-scale industrial production should be considered. To the best of our knowledge, complex, elaborate, and costly methods such as the sol-gel method, gel-casting, freeze drying, and the use of replica templates, have not been employed to fabricate lightweight aggregates. In addition, while a connecting structure of pores is set as a target for porous ceramics, a high closed porosity proportion is desired during the fabrication of lightweight aggregates.

2.2.1 Partial sintering

Partial sintering is the most used method to fabricate lightweight aggregates. As presented in Fig. 8, the main principle of this method is to stabilise the voids between the starting powder particles by adding certain additives [63]. The additives could be particles with smaller size and greater surface activity than the starting material, or sintering aids that can form a liquid phase during heat treatment. Using additives, the starting powder particles are necked, and thus, the voids remain in the material.

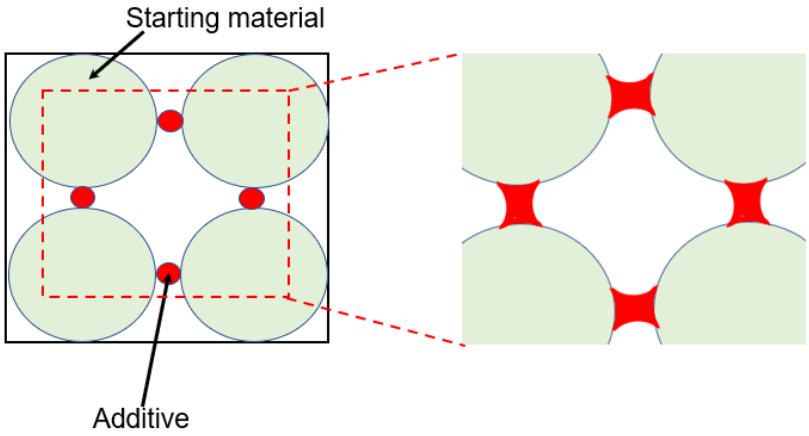

Fig. 8. Schematic diagram of partial sintering method. During in the sintering process, the particles of starting material are necked by the additives, resulting in the formation of stomatal structure.

The pore size and porosity of lightweight aggregates are significantly affected by the initial particle size of the starting materials and the heat treatment parameters used during fabrication [40]. In general, the final pore size is approximately in the range of 1/3−1/6 of the average starting powder size [64]. A narrow particle size distribution range of raw materials is helpful to fabricate lightweight aggregates with uniformly-distributed pore size. In addition, increasing forming pressure, sintering temperature, and soaking time reduces the porosity and pore size.

In the partial sintering technique, the addition of additives should be precisely controlled. It is difficult to stabilise the porous structure if the additives are added in low quantities; however, owing to their high surface activity and tendency to form a liquid phase the addition of an excess amount of additives may result in the sintering densification of lightweight aggregates [65]. Moreover, the grain coarsening (Ostwald ripening process) might occur during liquid phase sintering. With the formation of liquid phase, smaller grains might partially dissolve into the liquid phase and precipitate on the larger grains, leading to grain coarsening.

Lightweight bauxite materials were manufactured by introducing magnesia additive to adjust the liquid phase content during the sintering process. The introduction of magnesia resulted in increased amount of liquid phase during the heat treatment. Lightweight bauxite with an open porosity of 7.5% and a closed porosity of 15.6% could be obtained when the liquid phase content was approximately 17% [28].

As the formation of a liquid phase is detrimental to the high-temperature performance of lightweight aggregates, submicron or nano-additives are considered better options [66,67]. By adding nano-particles of alumina, zirconia, and magnesia, a series of lightweight alumina, bauxite, and magnesia aggregates were produced [26,29,31,68-71]. The addition of

nano-additives creates a large local curvature on the grain boundaries, which accelerates their migration, resulting in the formation of intracrystalline pores (Fig. 9). The introduction of intracrystalline pores led to a simultaneous improvement in the heat insulation, mechanical properties, and slag resistance of the fabricated lightweight aggregates [31]. Furthermore, with the addition of nano-alumina and zirconia in lightweight magnesia, intergranular phases of spinel and $CaZrO_3$ are formed in-situ and the degree of direct bonding between periclase grains was improved [70,71]. When a mixture of nano-additives and MgO/CaO powders was employed in the fabrication of lightweight alumina, an in-situ phase stress was produced during the reaction between nano-additives and MgO/CaO powders. Under phase stress, the pores closed and were divided by boundary migration, leading to increased closed porosity and reduced pore size [72]. By controlling the amount and type of nano-additives, the proportion of closed pores could be increased to 40−70%.

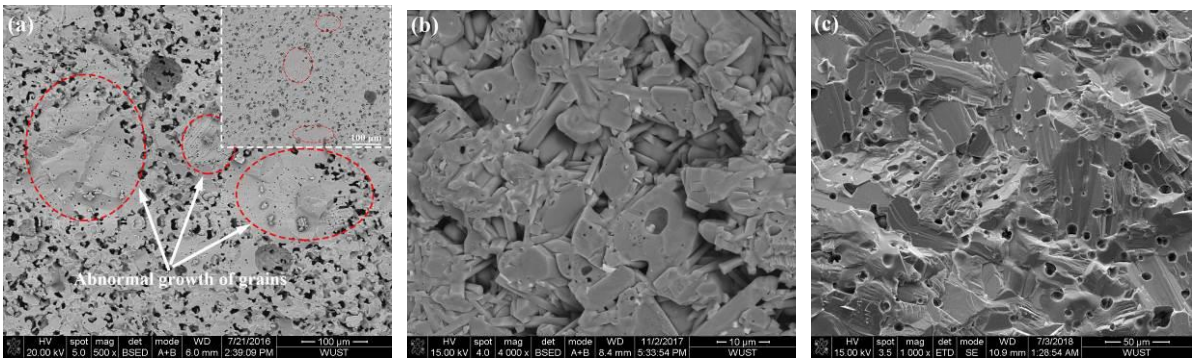

Fig. 9. SEM images of lightweight aggregates fabricated by the addition of nano-additives: (a) lightweight alumina, (b) lightweight bauxite, (c) lightweight magnesia. With the addition of nano-additives, the migration of grain boundaries is improved, leading to the formation of intracrystalline pores.

2.2.2 In-situ decomposition

The in-situ decomposition technique involves the use of decomposable inorganic matter such as hydroxides, carbonates, and hydrosilicates as raw materials. The decomposition of

these materials during the heat treatment process leads to volume contraction of the particles resulting in the formation of voids. Moreover, the products generated upon decomposition are fine particles with high surface activity. Owing to the good sinterability of the decomposition products, the porosity structure is stabilised [73,74].

The porosity morphology and properties of the lightweight aggregates thus produced are therefore affected by the type, addition, and particle size of raw materials and the technical parameters of the formation and sintering processes.

Li et al. [14], Salomão et al. [75] and Huang et al. [76] manufactured porous alumina-spinel materials using three different magnesium-containing minerals (basic magnesium carbonate, hydrotalcite, and magnesite) as raw materials. When compared to the other two raw materials, the higher impurity content in magnesite promotes the formation of a liquid phase during heat treatment. This leads to a better degree of bonding between the particles, resulting in improved mechanical strength and decreased pore size. This effect is particularly evident in the case of magnesite which contains higher contents of silica and alumina impurities.

The addition of decomposable raw materials during the fabrication of lightweight aggregates with a single-phase composition may be conducive to the improvement of mechanical properties. Deng et al. fabricated porous alumina using alumina and aluminium hydroxide as raw materials and discussed the effect of the amount of aluminium hydroxide on the mechanical properties of the product [73,74]. Although the porosity was comparable, the flexural strength and fracture toughness of porous alumina improved with an increase in the amount of aluminium hydroxide added. This improvement is a result of the high activity of alumina particles produced by aluminium hydroxide decomposition.

However, the influence of raw materials is more complex in the fabrication of lightweight

aggregates with multiple phases. The influence of the amount of decomposable raw materials used on the pore characteristics and properties of lightweight MgO-Al_2O_3, cordierite-mullite, periclase-spinel, and corundum-mullite materials were investigated in Ref. [77-81]. It is reported that the amounts of liquid phase and new phases are the two key factors affecting the pore morphology and properties of the fabricated lightweight aggregates. On the one hand, with increasing amount of generated liquid phase, the sintering process would be promoted, leading to reduction in pore size and porosity. On the other hand, volume expansion would be produced during the formation of new phases. When small amount of new phases is formed, this volume expansion might fill in the voids, which could reduce the pore size and porosity. However, excessive amount of new phases would hinder sintering densification, resulting in increased pore size and porosity. The amounts of liquid phase and new phases are heavily dependent on the content of decomposable raw materials, thus, the compositions of used raw materials should be strictly controlled. Moreover, decreasing the particle size of raw materials and increasing the sintering temperature both lead to smaller pore size and increased mechanical strength of the lightweight aggregates fabricated via in-situ decomposition technique [82-84].

The most important limitation of lightweight aggregates fabricated using the in-situ decomposition method is high open porosity, which results in unsatisfactory slag resistance and mechanical properties of materials. Therefore, several studies attempted to improve the slag attack resistance and strength. When the pressure employed in the process of forming the green body was increased, the closed porosity proportion could be increased slightly [85]. The mechanical properties were significantly improved by incorporating TiO_2 additives, which promote liquid phase formation. As shown in Fig. 10, lightweight alumina aggregates reinforced by in-situ formed SiC whiskers were fabricated [86-89]. The Al_2O_3-C refractory

prepared with these lightweight alumina aggregates showed a 30% higher flexural strength than that of the conventional dense Al_2O_3-C refractory.

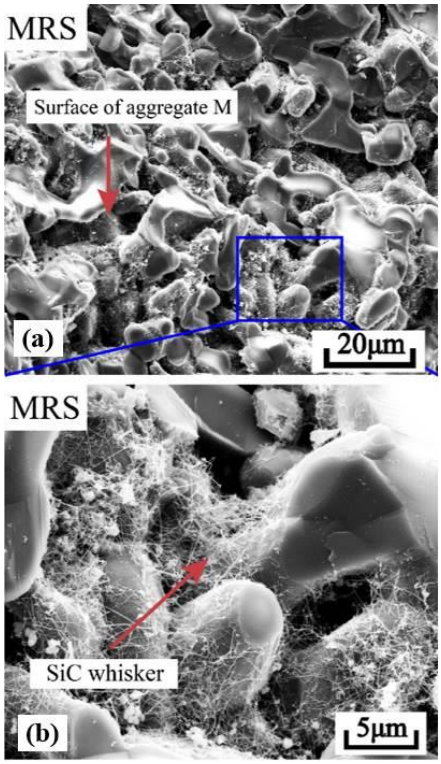

Fig. 10. Lightweight alumina aggregates reinforced by in-situ formed SiC whiskers. Due to the porous structure of lightweight alumina aggregates, vapor could easily diffuse into the micropores of the aggregates, and in-situ SiC whiskers are generated on the surface of lightweight aggregates.

Reprinted from Ref. [89], Copyright (2020) with permission from Wiley.

2.2.3 Addition of pore-forming agents

When pore-forming agents are added to the starting powder, they burn during the heat treatment process, leaving voids in the ceramic materials. When compared to other techniques, the use of pore-forming agents allows the porosity level of the fabricated materials to be easily controlled. In this case, a higher sintering temperature could be applied to the ceramic green body, which improves the mechanical strength of the fabricated lightweight materials.

The key factors in this technique are the type, addition, and particle size of the

pore-forming agent used.

Currently used pore-forming agents can be divided into two groups: organic materials and inorganic materials. Commonly used organic pore-forming agents include starch, rice husk, serrago, PMMA microspheres, and walnut shells [90-92], while commonly used inorganic materials include coal ash, carbon, and H_3PO_4 [93-95]. There is a clear association between the morphology of the pore-forming agent and the pores in the fabricated lightweight aggregates. Therefore, the fraction, size, and morphology of the pores are directly related to the pore-forming agent selected [49].

Porous alumina was fabricated using carbon black as a pore-forming agent by Liu et al., and the influence of pore structure on thermal conductivity and mechanical properties of porous alumina was discussed [96]. It was found that the heat insulation and mechanical strength of porous alumina could be enhanced by increasing the proportion of pores with a size below two micrometres. Fu et al. designed orthogonal experiments to assess the correlations among processing parameters and physical properties of lightweight alumina and pointed out that the total porosity of lightweight alumina is dependent on the amount of pore-forming agent added, while the sintering temperature influences the apparent and closed porosity of samples [40].

The addition of pore-forming agents is often used in combination with other techniques to fabricate lightweight aggregates with improved properties. As shown in Fig. 11 (a), lightweight bauxite was prepared by combining the use of a pore-forming agent and the partial sintering method [28]. By controlling the addition of the pore-forming agent and additives, lightweight bauxite with an average pore diameter of 0.82 μm and a closed porosity of 15.6% was fabricated. A combination of the pore-forming agent and impregnation method was adopted to improve the mechanical properties and pore structure of porous alumina [97]. As

presented in Fig. 11 (b), the pore structure in porous alumina could be modified after being impregnated with alumina sol, leading to enhanced mechanical properties and decreased thermal conductivity.

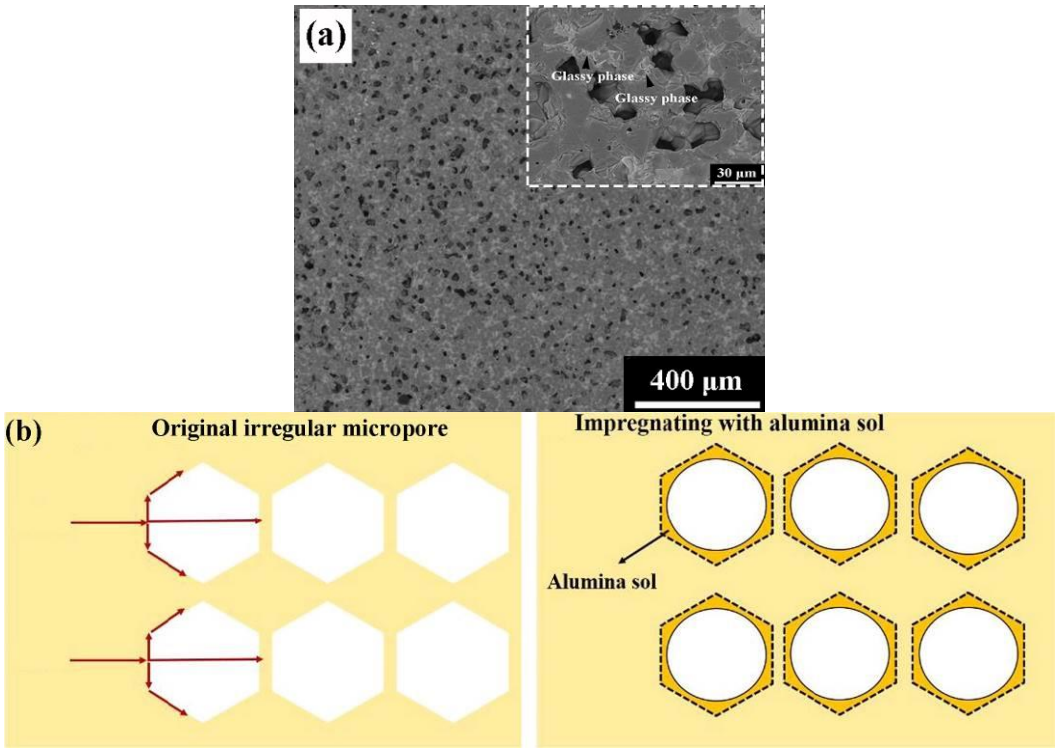

Fig. 11. (a) SEM images of lightweight bauxite prepared by combining the use of a pore-forming agent and the partial sintering method. (b) pore structure modification by impregnation with alumina sol. The pore structure is reinforced by alumina sol, resulting in improved mechanical properties.

Adapted from Refs. [28] and [97], Copyright (2018 & 2019) with permission from Elsevier.

2.2.4 Direct foaming

In the direct foaming technique, foams are first produced by frothing a mixture of foaming agent and water. The foams and raw material slurries are then mixed and formed, and the porous materials are obtained after drying and sintering. However, the chief disadvantage of this method is the large pore size. Generally, the average pore size of porous materials

manufactured using direct foaming is up to 200−300 μm [98-100]; these materials possess very low mechanical strength and exhibit poor resistance to slag attack. Therefore, porous materials fabricated using this method are applied in the insulation layer, rather than as wear linings.

To improve the slag resistance of foamed porous alumina, a lightweight alumina material with a core-shell structure was designed by Chen et al., as shown in Fig. 12 (a) [101]. A microporous shell was designed to protect the microporous core from slag attack. The macroporous core produced using the direct foaming method had a pore size of approximately 45−100 μm (Fig. 12 (b)). The microporous shell was fabricated using the partial sintering method with alumina powder as the raw material. After being sintered at 1800 °C, the microporous shell exhibited a small pore size of approximately 6−7 μm (Fig. 12 (b)). This lightweight alumina sphere showed an open and closed porosity of 10.9% and 13.6%, respectively. Using lightweight alumina sphere as aggregates, a lightweight alumina−magnesia castable was produced. When compared to the conventional dense alumina−magnesia castable, the lightweight castable showed a 21.4% lower thermal conductivity at 1000 °C and comparative slag attack resistance.

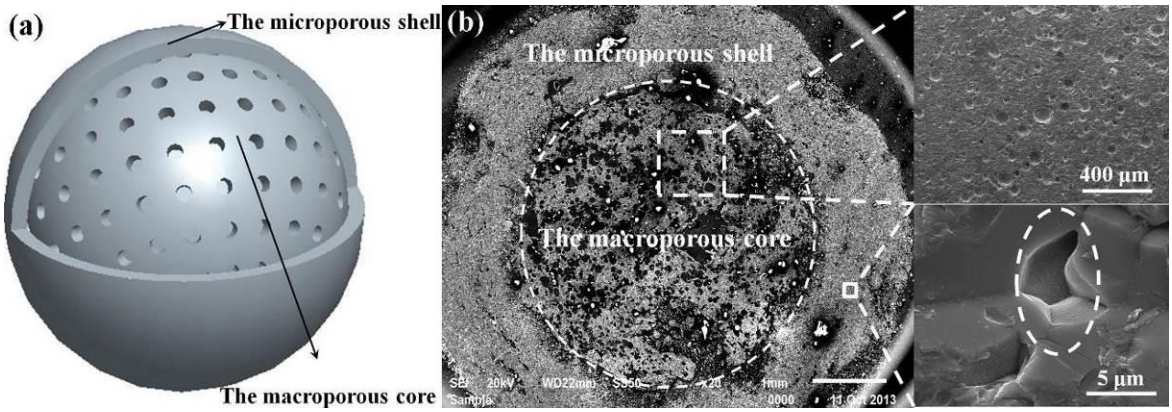

Fig. 12. (a) Schematic diagram and (b) SEM images of lightweight alumina with core-shell structure. It has a microporous shell and a macroporous core to achieve the

trade-off between thermal conductivity and corrosion resistance.

Adapted from Ref. [101], Copyright (2015) with permission from Elsevier.

2.2.5 Superplastic foaming

To produce lightweight materials with a high fraction of closed porosity and low fraction of open porosity, a novel route referred to as the 'superplastic foaming method' was proposed by Kishimoto et al. based on the superplasticity of ceramics [102]. Superplasticity is defined as the ability of a material to exhibit substantially large elongation under load, indicating that plastic deformation of ceramics may occur under application of stress.

First, suitable starting materials should be selected to produce a ceramic body with superplasticity at high temperature. In general, ceramic materials exhibit high-temperature superplasticity only when their grain size is smaller than 1 μm. Thus, the starting materials used are mainly nano-sized or submicron-sized powders. Second, this techniques requires the addition of high-temperature foaming agents, which are inorganic materials that are oxidized or decomposed at high temperature, such as SiC, Si_3N_4, and hydroxyapatite.

As shown in Fig. 13 (a), the starting material and high-temperature foaming agent are first compacted to obtain a green body. The green body is then sintered at a temperature lower than the oxidation or decomposition temperature of the high-temperature foaming agent to produce a dense ceramic bulk (Fig. 13 (b)). Then, the ceramic bulk is reheated at a higher temperature to generate gaseous species by the high-temperature foaming agent. Owing to the partial pressure of gases and the superplasticity of the ceramic matrix, closed pores are formed in the final ceramic material (Fig. 13 (c)).

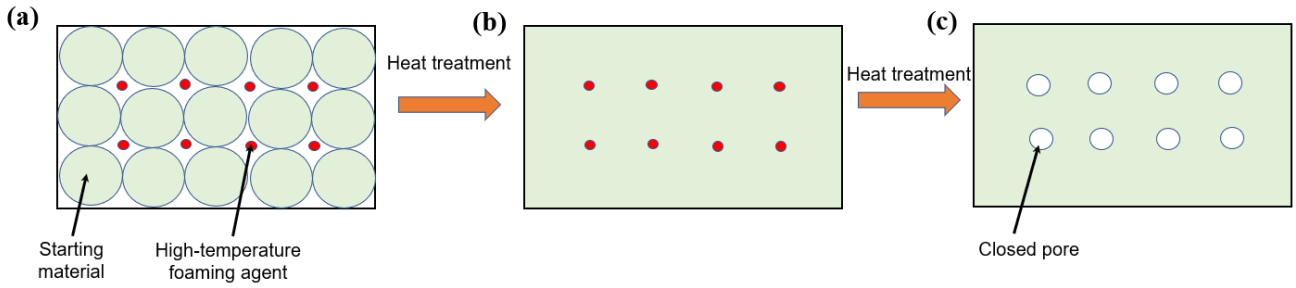

Fig. 13. Flow chart of fabrication of lightweight aggregates via superplastic foaming method. The green body is firstly sintered at a lower temperature to produce a dense ceramic bulk. The ceramic bulk is reheated at a higher temperature, with the decomposition of high-temperature foaming agent, closed pores are formed.

Until recently, the superplastic foaming method was mainly used to fabricate lightweight alumina and zirconia [102-108] owing to their good high-temperature superplasticity. The properties of the fabricated materials are mainly affected by the type, particle size, and amount of the starting material and high-temperature foaming agent. Furthermore, certain additives are introduced to improve the superplasticity of alumina and zirconia.

Lightweight zirconia was fabricated using nano-zirconia as the starting material and hydroxyapatite as the foaming agent [105]. By adding SiO_2 and TiO_2 additives, lightweight zirconia with a closed porosity of 24.6% and an open porosity of 2.1% was obtained. As shown in Fig. 14 (a) and (b), the sizes of the closed pores are mainly in the range of 10−20 μm. Lightweight alumina-based aggregates were prepared by adding MgO additive into submicron-sized alumina and SiC powder [108]. The introduction of MgO additive promoted the superplastic deformation of the alumina ceramic (Fig. 14 (c) and (d)). An increase in the amount of SiC forming agent and MgO additive resulted in the fabrication of lightweight aggregates with increased closed porosity.

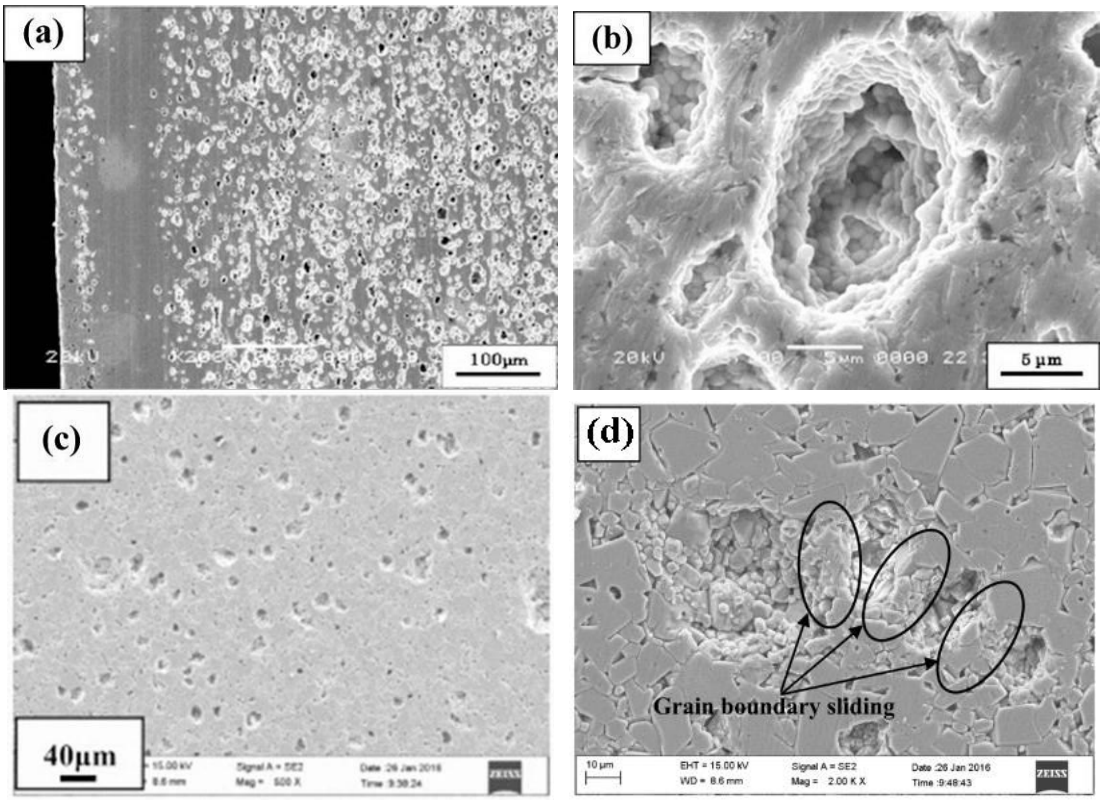

Fig. 14. SEM images of (a) and (b) lightweight zirconia, and (c) and (d) lightweight alumina produced via the superplastic foaming method.

Adapted from Ref. [105], Copyright (2013) with permission from Elsevier and Ref. [108], Copyright (2018) with permission from Taylor & Francis.

To facilitate better understanding of the properties of lightweight aggregates that are fabricated using various methods, a summary of the data reported in literature is listed in Table. 1. In-situ decomposition technique is the most economical method among all the process routes, however, the lightweight aggregates fabricated via in-situ decomposition technique typically possess high open porosities. Partial sintering and adding pore-forming agent methods offer easy and cheap ways to prepare lightweight aggregates with porosity below 20%. Direct foaming technique possess higher cost than the above-mentioned three methods. Superplastic foaming route has significant advantages in producing lightweight aggregates with high closed porosity. However, because the starting materials used are mainly nano-sized or submicron-sized powders, the cost of superplastic foaming is the highest.

Table 1. Summary of the data reported in literature on properties of lightweight aggregates fabricated using various methods

Composition	Processing method	Open porosity	Closed porosity	Pore size	References
Alumina	Adding pore-forming agent	3.4−15.2%	2.8−12.6%	1−10 μm	[40]
Alumina	Adding pore-forming agent + partial sintering	5.2−10.5%	7.1−12.3%	Average: 0.1−1.5 μm	[26,27,65,68,69,72]
Alumina	In-situ decomposition	25.7%	3.2%	Average: 4.2 μm	[89,109]
Alumina	Direct foaming	10.9%	13.6%	Average: 6.47 μm	[101]
Corundum-spinel	In-situ decomposition	35−40%	-	Average: 3−11 μm	[14,19,79]
Corundum-spinel	Superplastic foaming	1−3%	13−15%	1−14 μm	[108]
Spinel	In-situ decomposition	40−60%	-	Average: 2.5−6.5 μm	[15,81,86]
Magnesia	In-situ decomposition	33.3%	0.2%	Average: 2.97 μm	[110]
Magnesia	Adding pore-forming agent + partial sintering	2−4%	6−7%	Average: 2−5 μm	[29,30,70,71]
Periclase-spinel	In-situ decomposition	30−45%	-	16−75 μm	[78]
Bauxite	Adding pore-forming agent + partial sintering	7.5%	15.6%	Average: 0.82 μm	[28]
Corundum-mullite	In-situ decomposition	30−45%	-	Average: 0.5−6 μm	[38,79,111,112]
Cordierite-mullite	In-situ decomposition	30−45%	-	50−120 μm	[39,77,80,84,91]
Zirconia	Superplastic foaming	2.1%	24.6%	10−20 μm	[105]

3. Lightweight wear lining refractories

In the following section, the particle packing of the matrix and density gradient design of lightweight wear lining refractories are discussed, and the factors influencing the wear lining refractories and their application are summarized.

3.1 Matrix particle packing design

The key factors that determine the lifespan of lightweight wear lining refractories are their mechanical properties and slag resistance. The matrix is often the weakest component susceptible to slag and stress, which is attributed to its higher porosity than that of the aggregates. Therefore, packing of particles in the matrix plays a critical role in the performance of refractories, particularly in lightweight refractories containing lightweight aggregates.

As shown in Equations (2) and (3), the Andressen and Dinger−Funk models are the most widely-accepted classical models for modelling the particle packing design of the refractory matrix [113].

$$CPFT = 100(\frac{d}{D})^n \tag{2}$$

$$CPFT = 100\frac{d^q - d_m^q}{D^q - d_m^q} \tag{3}$$

However, the complete particle size distribution, particularly for particles smaller than 88 μm, is difficult to accurately described using classical models. A novel particle packing design model was proposed by Zou et al. to predict the packing density of lightweight refractories [114]. The particle size distribution of the matrix was divided into *N* groups, and the volume percentage of each group was calculated from the measured particle size distribution of each component. The particle packing density, *P*, could be predicted using Equations (4) and (5) [114].

$$P = \min\left\{P_1, P_2, ..., P_n, ..., P_N\right\} \tag{4}$$

$$P_n = \frac{P_{n,0}}{1 - \sum_{m=1}^{m=n-1}\left[1 - P_{i,0} + w(r)P_{i,0}(1 - 1/P_{j,0})\right]X_m - \sum_{m=n+1}^{N}\left[1 - l(r)P_{i,0}/P_{j,0}\right]X_m} \tag{5}$$

Based on the results, the relative packing densities of lightweight alumina–magnesia castables with different critical size and q-value were calculated. As shown in Fig. 15, the packing density reaches a maximum with a critical size of 8 mm and q-value of 0.28. To verify the reliability of this model, lightweight alumina–magnesia castables with different q-values were fabricated by Zou et al., and the microstructures and properties of castables were compared.

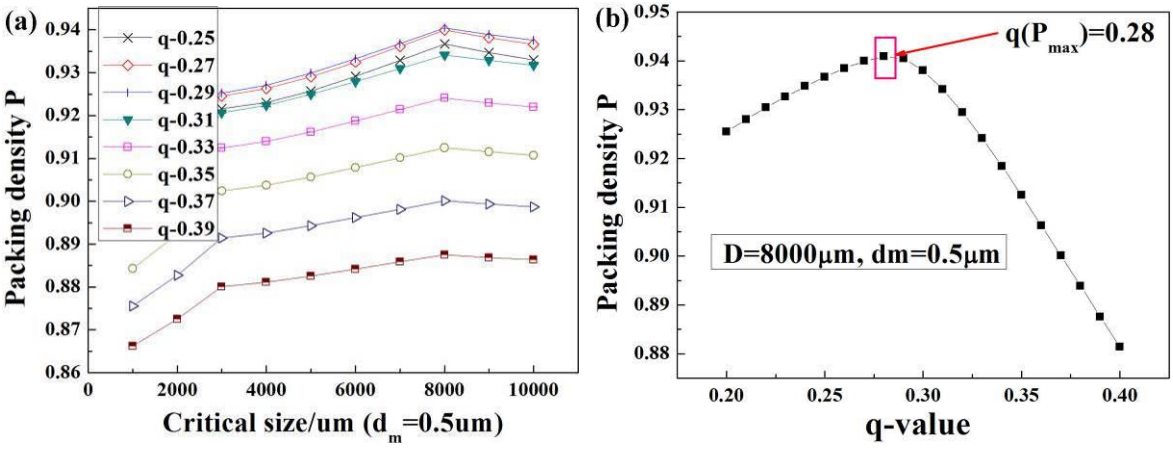

Fig. 15. Relative packing density of lightweight refractories with different (a) critical size and (b) q-values. The maximum theoretical packing density can be reached when a critical size of 8000 μm and a q-value of 0.28 is chosen.

Reprinted from Ref. [114], Copyright (2016) with permission from Elsevier.

As presented in Fig. 16, the sample with a q-value of 0.28 showed a denser matrix and better bonding degree between the matrix and aggregates compared to other samples. The slag resistance performance of various castables were assessed using static crucible method. The results indicated that the sample with a q-value of 0.28 exhibited the best resistance to slag

corrosion and penetration [34,114].

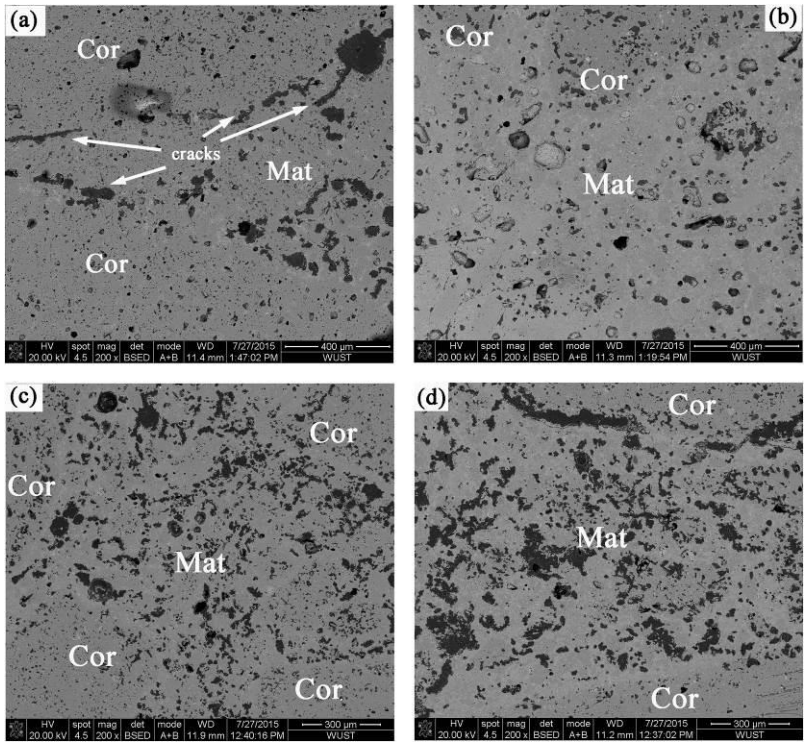

Fig. 16. SEM image of lightweight alumina–magnesia refractories with different q-value: (a) 0.25, (b) 0.28, (c) 0.31, (d) 0.34. (Cor=lightweight aggregates, Mat=matrix). Reprinted from Ref. [114], Copyright (2016) with permission from Elsevier.

3.2 Refractories with density gradient

Yin et al. proposed a novel method based on the carbothermal reduction of MgO to fabricate lightweight refractories without the addition of lightweight aggregates [36,37]. As shown in Fig. 17 (a), tabular alumina was selected as the aggregate, while the matrix was composed of powders of fused magnesia, alumina, and graphite. The green body was heated at 1550 °C for 4 h in an electric furnace, and the atmosphere in the electric furnace was changed during the heat treatment process. An argon atmosphere was applied during the heating stage; after the temperature reached 1550 °C, the atmosphere was switched to pure oxygen. As shown in Fig. 17 (b), the carbothermal reduction of MgO occurs during the heating stage. The generated Mg vapour diffuses to the surface of the refractory, and voids are left in the inner

region of the material. Upon changing the atmosphere, spinel is formed owing to the reaction between oxygen and Mg vapour. Therefore, a lightweight corundum–spinel refractory with a density gradient was produced.

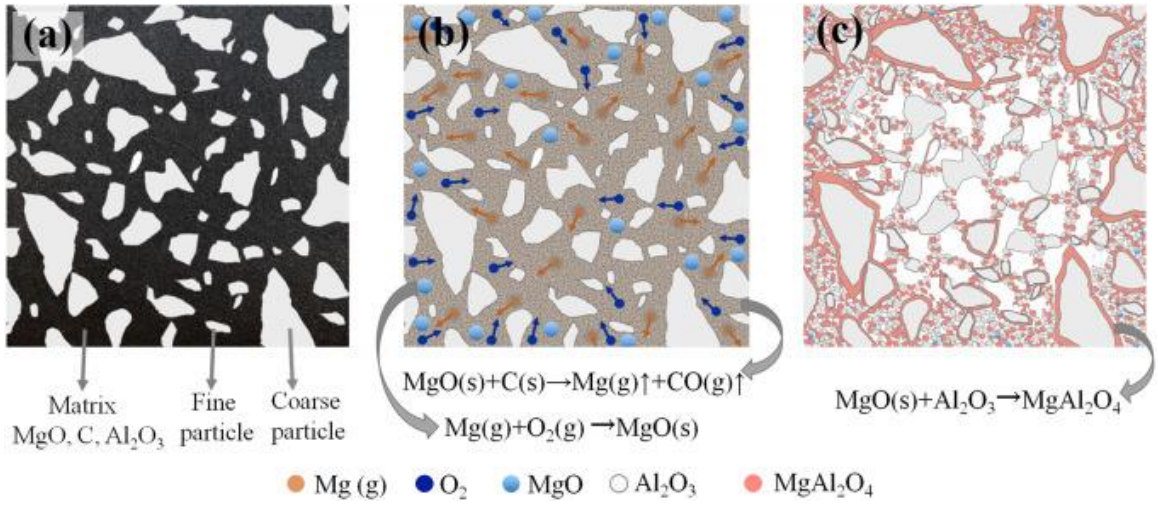

Fig. 17. Schematic diagram of the production of lightweight refractories with gradient density. Mg vapour would be generated and diffuse to the surface of the refractory during the carbothermal reduction of MgO. With the atmosphere being switched to pure oxygen, a lightweight refractory with a density gradient could be obtained. Reprinted from Ref. [36], Copyright (2019) with permission from Elsevier.

The density variation in two lightweight corundum–spinel refractories with the density gradient is shown in Fig. 18 [37]. The density difference of approximately 0.15 g/cm^3 was detected between the surface and centre of the produced lightweight refractories. Owing to the density of the surface, the lightweight refractories showed slag resistance comparable to that of the conventional dense corundum–spinel refractory [115]. Furthermore, the microstructures and properties of lightweight corundum–spinel refractories were affected by the carbon source, additives, and heat treatment [116-120].

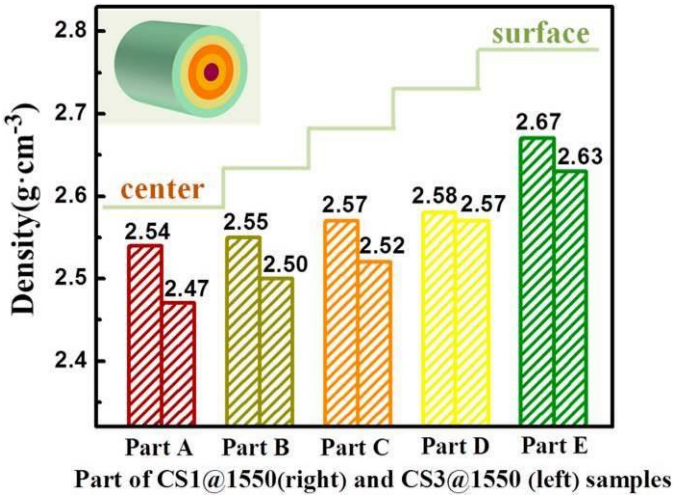

Fig. 18. Density variation of different lightweight refractories with gradient density. The densities of refractories are gradually increased from the centre to the surface. Reprinted from Ref. [37], Copyright (2018) with permission from Elsevier.

3.3 Materials characterization

In general, the current characterization and modeling methods for refractories could also be used for lightweight refractories. Since the properties of lightweight refractories are directly determined by the porosity morphology, an understanding of complete information on porosity morphology is essential. The main difficulty is the characterization of closed pores. Indeed, classical characterization techniques (scanning electron microscope, mercury intrusion porosimetry method) could hardly identify the structural characteristics of closed pores.

To obtain quantitative information about pore morphology, X-ray tomography technique has been frequently employed in the characterization of lightweight refractories [121-123]. With the application of image processing and analysis software, the produced projections during the scanning are compiled and a 3D reconstruction of the material could be obtained. Fig. 19 presents reconstructed 3D pore structures of lightweight Al_2O_3-SiO_2 materials [121]. As shown, the particular information on porosity morphology (open/closed porosity, pore size, pore interconnectivity, and pore shape) could be quantificationally obtained. In addition, since

it is a non-destructive method, it allows to investigate the change in pore morphology during heat treatment.

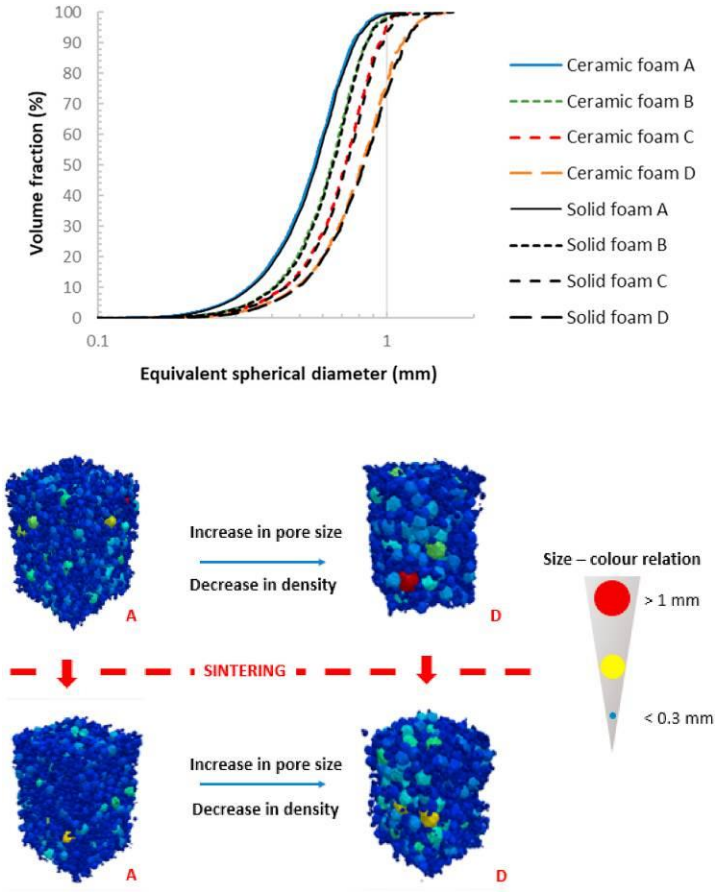

Fig. 19. Porosity morphology of lightweight Al_2O_3-SiO_2 materials explored using X-ray tomography technique. The graph at the top of the figure provides the pore size distribution and the bottom graphs present the reconstructed 3D pore structures before and after sintering.

Reprinted from Ref. [121], Copyright (2020) with permission from Elsevier.

3.4 Factors affecting the properties of fabricated lightweight refractories

As a high-temperature material containing complex compositions in phase, chemical component, and particle size, the properties of the refractory are affected by many internal and external factors. In the following section, factors that affect the properties of lightweight

refractories are summarised and discussed in detail.

3.4.1 Materials composition

The chemical and phase compositions of lightweight aggregates play a key role in the properties of fabricated lightweight refractories, especially in the case of lightweight aggregates with composite phases. Porous spinel aggregates containing different Al_2O_3 content (57.6 wt%, 71.1 wt%, and 87.7 wt%) were selected to produce alumina−magnesia castables by Yan et al., and the slag resistance performance of different castables were compared [124]. With an increase in the Al_2O_3 content in the porous spinel aggregate, the fabricated castable showed improved resistance to slag penetration and reduced slag corrosion resistance [125].

Lightweight periclase−spinel refractories were fabricated using different porous periclase−spinel aggregates, and the effect of spinel content on the properties of lightweight refractories were investigated in Ref. [126,127]. An increase in the spinel content in the aggregates led to a consequent increase in the amount of liquid phase formed during the reaction between the refractory and cement clinker. The amount of liquid phase should be within a suitable range to achieve a good bonding degree between the refractory and cement clinker. As shown in Fig. 20, the fabricated lightweight refractory exhibited satisfactory adherence and slag resistance when the spinel content of the lightweight aggregates was in the range 15−40 wt%.

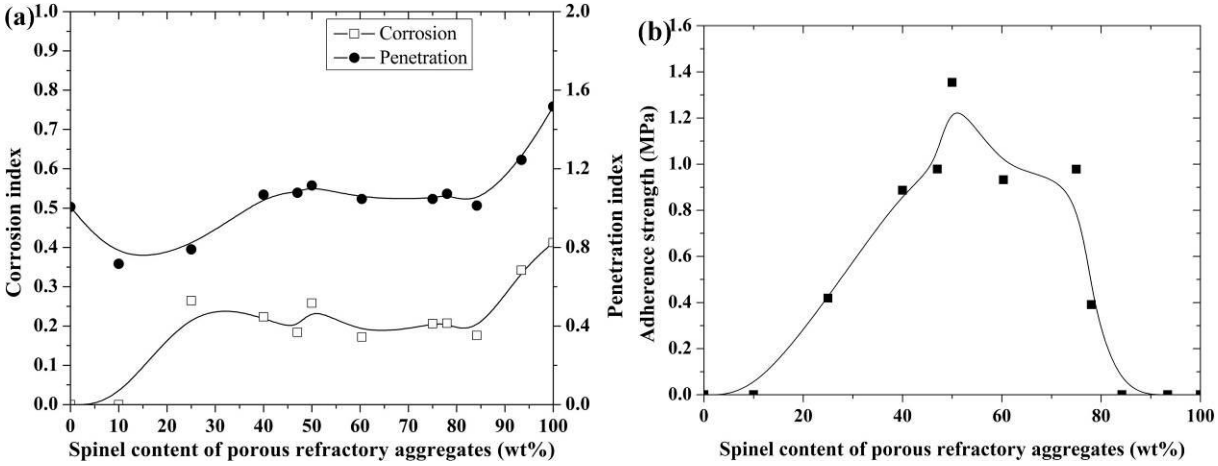

Fig. 20. (a) Slag resistance and (b) adherence strength of lightweight refractories containing porous aggregates with different spinel content. Adherence and slag resistance of the fabricated lightweight refractory are strongly affected by the spinel content of the lightweight aggregates.

Reprinted from Ref. [126], Copyright (2017) with permission from Elsevier.

In addition, the properties of lightweight magnesia aggregates were improved by modifying the intergranular phase composition. By adding nano-powder of alumina and zirconia, in-situ intergranular phases of spinel and calcium zirconate were formed in lightweight magnesia, resulting in improved slag resistance and reduced thermal conductivity [70,71]. Several attempts have also been made to improve the matrix by the addition of additives. Powders of light-burned spinel, SiC, spinel, and microsilica have been introduced to enhance the bonding degree between the matrix and aggregates [128-131].

3.4.2 Structural characteristics

As mentioned in Section 2.1, the porosity characteristics significantly affect the properties of lightweight aggregates. Slag corrosion tests were conducted on various lightweight alumina aggregates to understand the effect of porosity on the slag resistance performance of lightweight aggregates [32]. When compared to the effect of open porosity,

pore size showed a higher correlation with the slag resistance of lightweight aggregates. Fu et al. proposed a reaction mechanism between molten slag and lightweight alumina, as shown in Fig. 21 [33]. When the alumina aggregate exhibits a small pore size, the second phase is more likely to achieve supersaturation; hence, a continuous isolation layer is formed on the interface between alumina and molten slag.

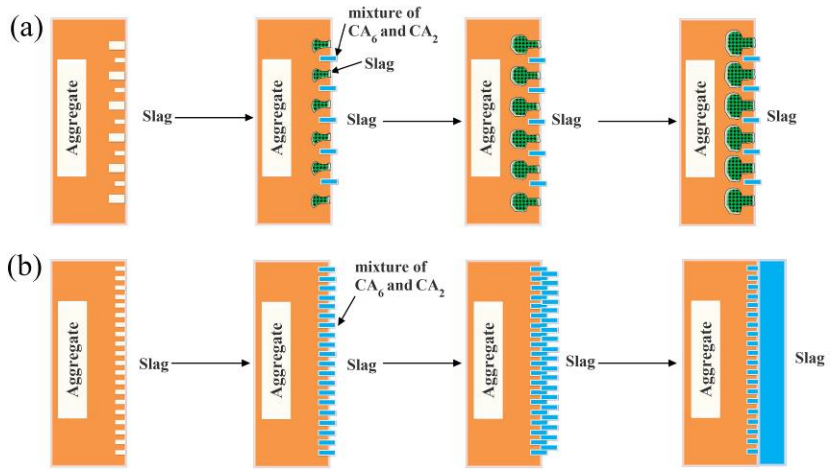

Fig. 21. Schematic diagram of the reaction between molten slag and lightweight alumina aggregates with (a) large and (b) small pores. For the lightweight aggregate with small pore size, the supersaturation of molten slag will be easily achieved. Solid phase will consequently precipitate out, converting a direct dissolution into an indirect dissolution. Reprinted from Ref. [33], Copyright (2015) with permission from Wiley.

Furthermore, the effect of the porosity characteristics of lightweight aggregates on the properties of fabricated lightweight refractories has been investigated [132-134]. Lightweight periclase−spinel castables were prepared using lightweight magnesia aggregates with different open porosity (12.8%, 30.8%, and 39.3%) by Yan et al. [133]. The bonding degree between the matrix and aggregates improved owing to the high open porosity. However, a very high open porosity results in the formation of cracks on the bonding interface between aggregates and matrix, and the mechanical properties decreased instead. Zou et al. found that the size and

shape of grains in lightweight aggregates play an important role in the slag corrosion behaviour of lightweight refractories [134].

The shape of lightweight aggregates is another important factor. As shown in Fig. 22, spherical lightweight mullite aggregates were produced by Yi et al. [135]. The particle packing of mullite−corundum refractory could be modified by introducing 45−65 wt% spherical aggregates, thus leading to improved mechanical properties [136].

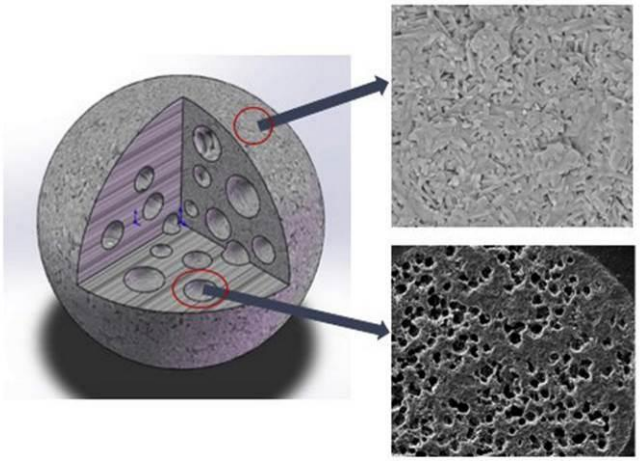

Fig. 22. Schematic and SEM images of spherical lightweight mullite aggregates. It has a porous internal structure and dense surface.

Reprinted from Ref. [135], Copyright (2019) with permission from Elsevier.

3.4.3 Atmospheric conditions

With the development of metallurgy technology, refractory linings are subject to changing service atmospheric conditions. The corrosion of alumina, mullite, magnesia, and zirconia refractories in gas environment (carbonaceous atmosphere, water vapor, hydrogen, and oxygen) was discussed by Mahapatra [137], who pointed out that the degradation of oxide refractories would occur when the partial pressure of volatile species is higher than 10^{-6} atm. In the atmospheres of carbonaceous gas (CO, CO_2, and hydrocarbon) and hydrogen, evaporation of silicon and aluminum volatile species would occur, leading to corrosion of

oxide refractories [138]. The recession of refractories would be further accelerated for atmospheres containing water vapor. As shown in Fig. 23, the reaction between alumina and water vapor would occur even in an oxidizing atmosphere. As for the non-oxide refractories (SiC, Si_3N_4), a mixture of oxidizing atmosphere and water vapor is more harmful [139].

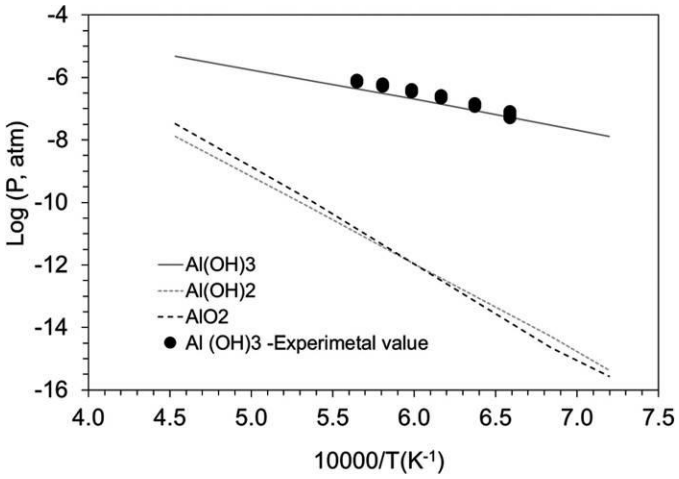

Fig. 23. Equilibrium partial pressures of aluminum vapor species from alumina in an atmosphere containing 0.5 atm oxygen and 0.5 atm water vapor.

Reprinted from Ref. [137], Copyright (2020) with permission from Wiley.

The slag resistance performance of lightweight alumina−magnesia castable under different atmospheric conditions was investigated by Zou et al. [140]. Dynamic induction furnace corrosion tests were conducted in weak oxidizing atmosphere ($P(O_2)$=0.21 atm) and argon atmosphere (P(Ar)=1.0 atm), respectively. As shown in Fig. 24 (a) and (b), when compared to weak oxidizing atmosphere, the argon atmosphere alleviated slag corrosion in the lightweight refractory. The form in which Fe and Mn ions exist in the molten slag is the main factor leading to the different slag reaction behaviour of lightweight castables. As presented in Fig. 24 (c), the Fe and Mn ions in the slag were reduced to elementary substances in argon atmosphere, leading to attenuated slag corrosion.

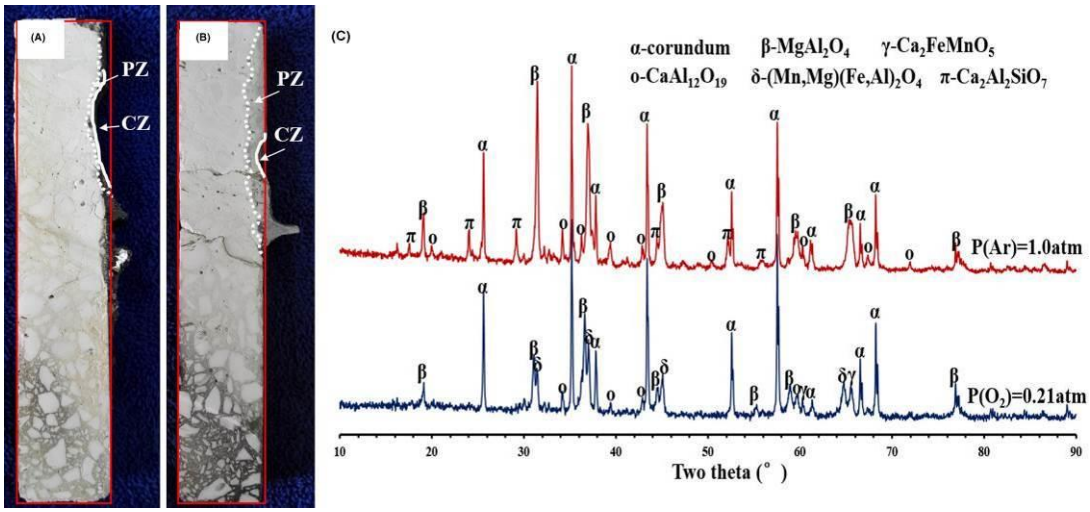

Fig. 24. Morphology of lightweight refractories after slag corrosion test at (a) P(O_2)=0.21 atm and (b) P(Ar)=1.0 atm, and (c) phase composition of corrosion area of refractories. Slag corrosion in the lightweight refractory was weakened in the argon atmosphere. Adapted from Ref. [140], Copyright (2018) with permission from Wiley.

3.4.4 Slag compositions

Refractories exhibit different resistances to molten slags with different chemical compositions. To understand the intrinsic reaction mechanism between lightweight aggregates and molten slags, four lime−alumina−silica slags with different chemical compositions were designed to assess the slag resistance of lightweight alumina aggregates [32]. As shown in Fig. 25, the dissolution rate of lightweight alumina and the viscosity of the molten slag were mainly affected by the chemical composition, leading to differences in slag reaction behaviours. The competition between alumina dissolution rate and solid phase precipitation rate is the key factor that determines the reaction behaviour. By controlling the relationship between the rate of these reactions, an isolation layer of calcium aluminates could be formed on the reaction interface between alumina and slag, protecting the aggregates from further slag attack.

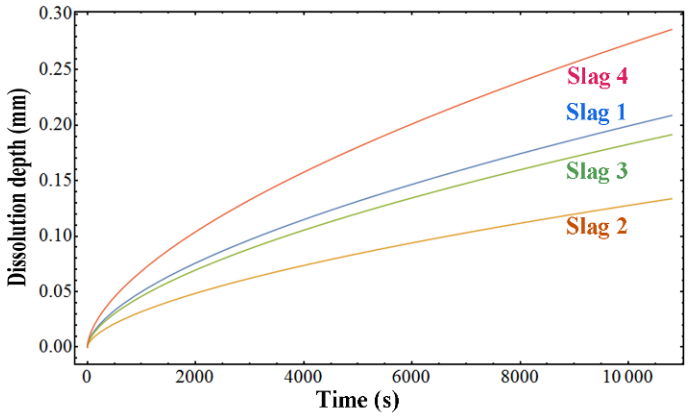

Fig. 25. Dissolution rate of lightweight alumina into various lime−alumina−silica slags. The viscosity of the molten slag has a critical influence on the slag resistance of lightweight alumina. When reacting with various molten slags, a balance between the alumina dissolution rate and the solid phase precipitation rate should be achieved to form an isolation layer.

Reprinted from Ref. [32], Copyright (2017) with permission from Elsevier.

The reaction between lightweight Al_2O_3–MgO castable and three different types of molten slags (Al_2O_3–CaO–SiO_2 slag, Al_2O_3–CaO slag, and Al_2O_3–CaO–SiO_2–MgO slag) were studied. As shown in Fig. 26, the Al_2O_3–CaO–SiO_2 slag strongly corroded both the aggregates and matrix of lightweight refractories, while Al_2O_3–CaO slag mainly corroded the matrix. Owing to the low content of the liquid phase formed during the reaction, the matrix and aggregates exhibited good resistance to Al_2O_3–CaO–SiO_2–MgO slag.

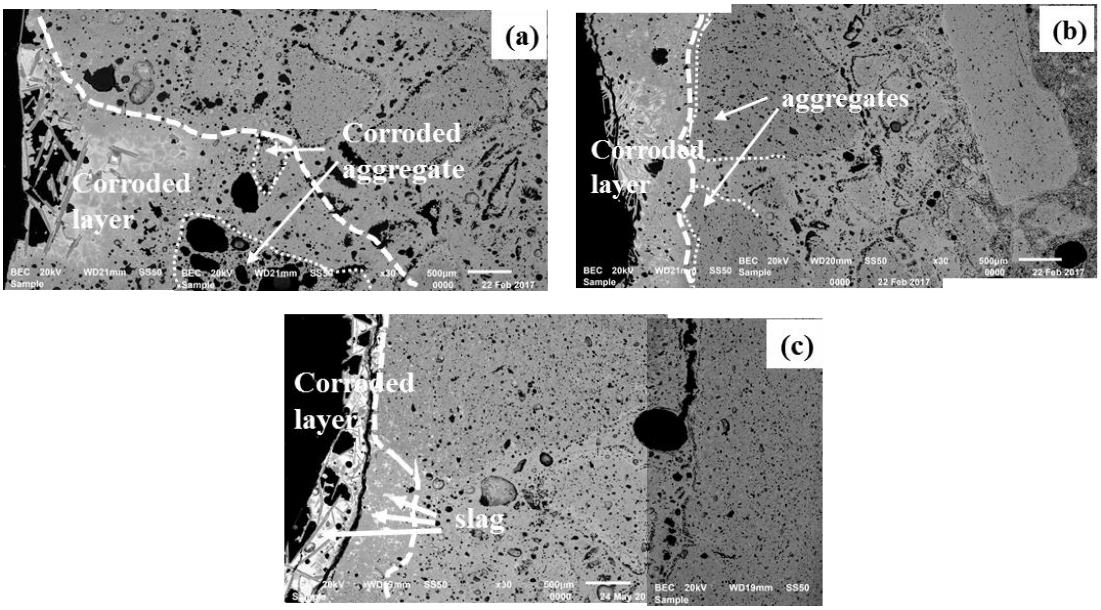

Fig. 26. Reaction interfaces between lightweight refractories and (a) Al_2O_3-CaO-SiO_2 slag, (b) Al_2O_3-CaO slag, and (c) Al_2O_3-CaO-SiO_2-MgO slag. Under dynamic slag corrosion condition, the chemical compositions of slag dominate the corrosion behaviour of lightweight refractories.

3.4.5 Electromagnetic fields

Electromagnetic fields are typically used in high-temperature industries for heating or stirring purposes. As there are large amounts of free movable ions and ionic groups in molten slag, it is conductive at high temperature. Therefore, the mass transfer between the refractory and molten slag changes significantly under the application of an electromagnetic field. The effect of an electromagnetic field on the reaction behaviour between MgO-based refractories and molten slags was studied by Aneziris et al. [141]. The contact angle and phase composition of the reaction layer was significantly influenced by the application of voltage.

The application of electromagnetic field significantly influences the slag corrosion process of lightweight refractories, considering their high porosity. Zou et al. found that the migration of ions and oxides of Fe and Mn increased under an alternating magnetic field, resulting in deeper slag corrosion and penetration of lightweight alumina−magnesia castables

[142]. However, the slag resistance of lightweight refractories was improved using a static magnetic field. Huang et al. assessed the slag resistance performance of lightweight alumina−magnesia castable under a static magnetic field, and the effect of magnetic strength was investigated [143]. With an increase in the magnetic induction intensity, the viscosity and contact angle of slag subsequently increased. Therefore, the slag attack was reduced. The reaction mechanism between lightweight magnesia and molten slags under a static magnetic field was proposed by Zou et al. [144]. As shown in Fig. 27, a Lorentz force was generated, attributed to the "electromagnetic braking" effect, hindering the movement of molten slags. As a result, the flow velocity and wetting ability of the slag reduced, leading to decreased slag penetration and dissolution rate.

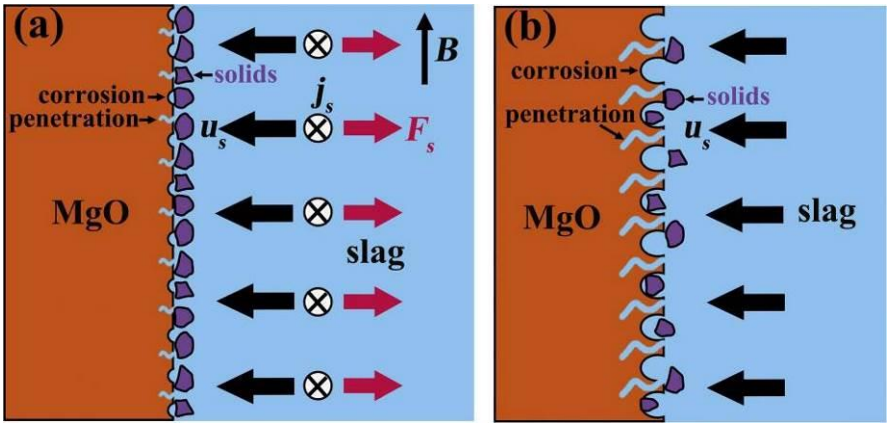

Fig. 27. Schematic diagram of slag corrosion behaviour (a) with and (b) without static magnetic field. With the application of static magnetic field, a Lorentz force was created during the slag flow process, resulting in decreased slag flow velocity and alleviated slag corrosion.

Reprinted from Ref. [144], Copyright (2020) with permission from Elsevier.

3.5 Performance and applications of lightweight refractories

The application of lightweight refractories in wear linings was first proposed by Chen et al. in 2003 [13]. Lightweight corundum−spinel castables were prepared by introducing porous

aggregates, and the properties of a dense castable and lightweight castable were compared. The lightweight castable showed a 32% lower thermal conductivity compared to a conventional dense castable. However, the slag attack area was 26.5% higher, indicating worse slag resistance. Moreover, the mechanical strength of the fabricated lightweight castable was unsatisfactory.

Since then, several attempts have been made to improve the lifespan of lightweight refractories by modifying the porosity characteristics and phase composition. The key target was to fabricate lightweight wear lining refractories with low thermal conductivity and guaranteed lifespan [145,146]. By setting conventional dense refractories as the references, the potential applications of fabricated lightweight refractories were evaluated.

By optimising the phase compositions and reducing the pore size of lightweight aggregates, lightweight corundum and periclase−spinel refractories with high mechanical strength were obtained [109,147,148]. Lightweight periclase−spinel refractory was fabricated using porous periclase−spinel (an open porosity of 23.3% and a median pore size of 5.66 μm) as aggregates by Yan et al. [147]. When compared to the dense periclase−spinel refractory, the lightweight refractory exhibited an 18.8% lower thermal conductivity, and 80.7% and 136.8% higher flexural strength after being fired at 1100 °C and 1600 °C, respectively. This is mainly due to the better bonding degree between lightweight aggregates and matrix (Fig. 28). Furthermore, the crack propagation paths in different castables were counted. As shown in Fig. 29, the proportion of transgranular fracture in the lightweight castable was significantly higher than that of the dense castable, resulting in improved mechanical strength [148]. However, owing to the high open porosity of porous aggregates, the slag resistance of the lightweight periclase−spinel castable was slightly worse than that of the dense refractory.

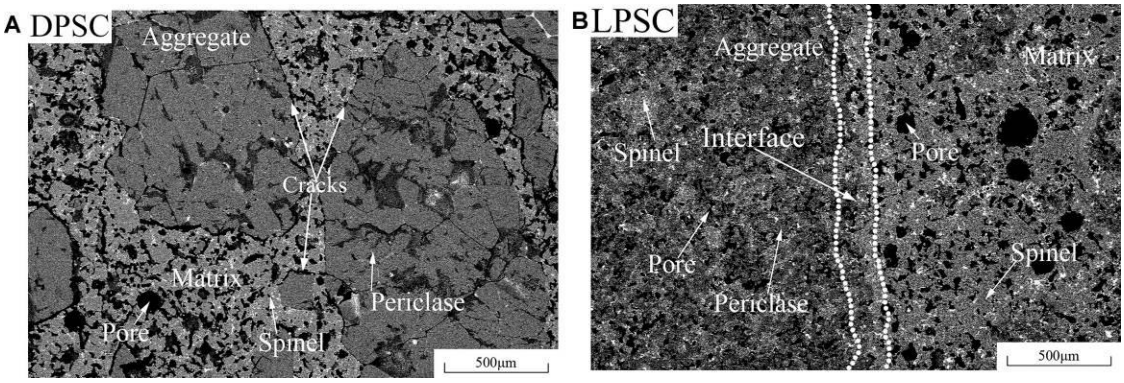

Fig. 28. Bonding interfaces between aggregates and matrix: (a) dense periclase–spinel castable (DPSC) and (b) lightweight periclase-spinel castable (LPSC). A good bonding degree between the matrix and aggregates has been formed in the LPSC. Reprinted from Ref. [147], Copyright (2018) with permission from Elsevier.

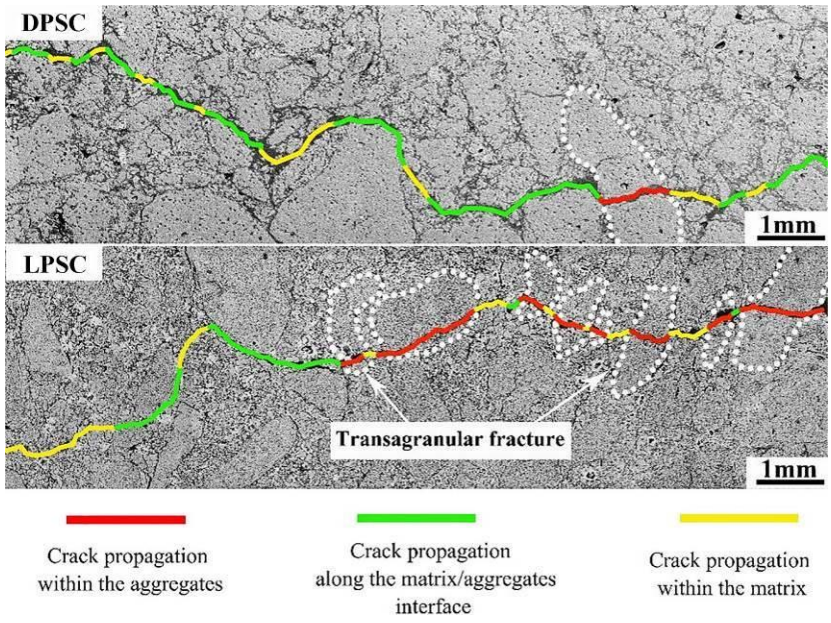

Fig. 29. Crack propagation paths in dense periclase–spinel castable (DPSC) and lightweight periclase–spinel castable (LPSC). The proportion of transgranular fracture in the lightweight castable was significantly higher than that of the dense castable. Reprinted from Ref. [148], Copyright (2021) with permission from Elsevier.

Several lightweight aggregates with high closed porosity and small pore size were manufactured to further increase the lifespan of the lightweight refractories [149-152].

Lightweight alumina with a bulk density of 3.36 g/cm^3 and closed porosity of 11.0% was fabricated by Hisashi et al. [149]. Lightweight and dense Al_2O_3-MgO-C bricks were then prepared using lightweight alumina and dense alumina as aggregates, respectively. The lightweight brick exhibited a 20% lower thermal conductivity and a lifespan similar to that of the dense brick. Using lightweight alumina with a bulk density of 3.36 g/cm^3 and closed porosity of 10.1% as the aggregate, a lightweight alumina−magnesia castable was produced by Fu et al. [23]. Besides a decreased thermal conductivity and increased mechanical strength, the lightweight castable demonstrated improved slag resistance (Fig. 30 (a) and (b)). As shown in Fig. 30 (c) and (d), owing to the small pore size of the lightweight alumina, the second phase easily precipitated and formed an in-situ isolation layer between the lightweight alumina and molten slag [33]. Consequently, the lightweight materials showed better slag resistance. Moreover, the cleanness of bearing steels could be improved using lightweight alumina−magnesia castable as the wear lining [153,154].

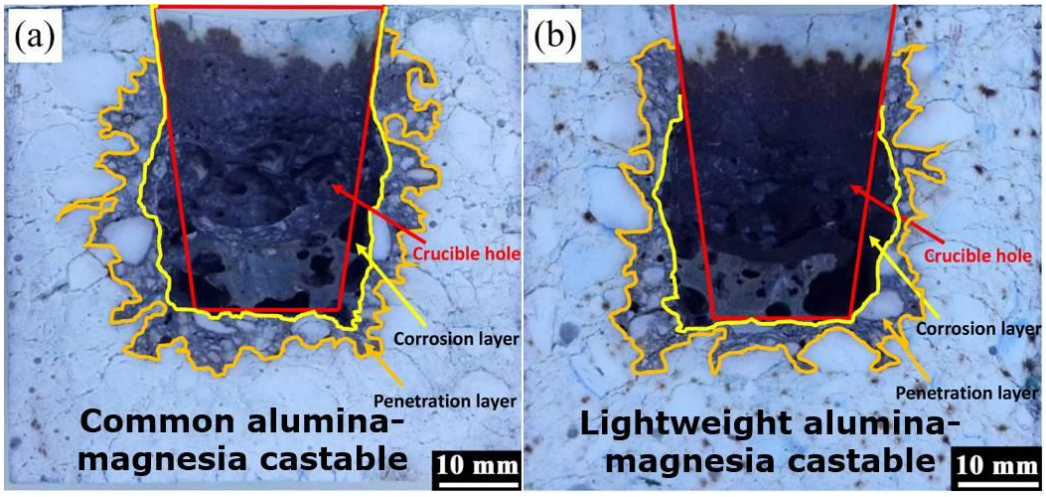

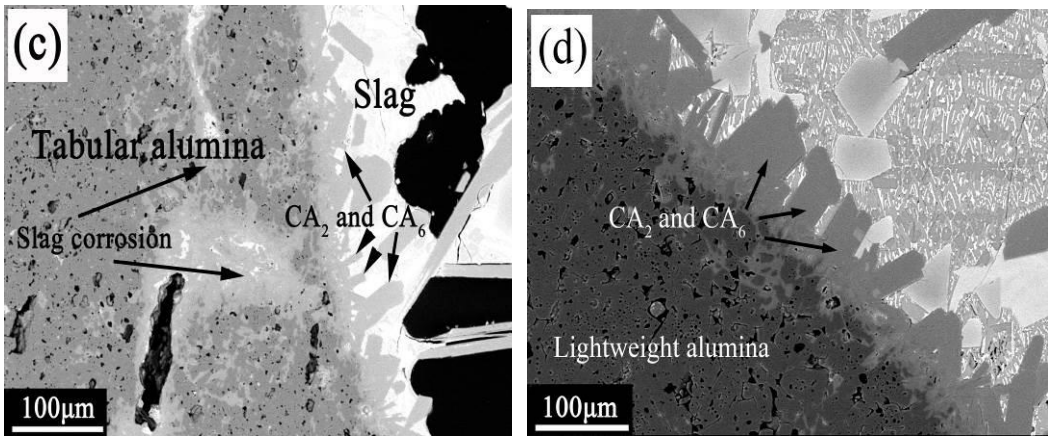

Fig. 30. (a) Common and (b) lightweight alumina−magnesia castable after slag corrosion test; reaction interface between molten slag and (c) tabular alumina and (d) lightweight alumina. Due to the small pore size of lightweight alumina aggregates, an in-situ isolation layer was formed to prevent them from further slag attack. Hence, the lightweight alumina-magnesia castable exhibited better slag resistance performance than the common castable.

Adapted from Ref. [23], Copyright (2015) with permission from Elsevier and Ref. [33], Copyright (2015) with permission from Wiley.

Lightweight corundum−spinel castables with a guaranteed lifespan have also been reported in Ref. [101,115,146]. Thus, briefly, the trade-off between thermal insulation and service life might be achieved by developing superior lightweight wear lining refractories. The key lies in the optimisation and control of the compositions, and structural characteristics and service conditions of lightweight refractories.

4. Conclusions and perspectives

The design of lightweight wear linings is important for the energy and resource efficiency of industrial furnaces and the quality of the final products. Lightweight wear lining refractories are generally fabricated by replacing conventional dense aggregates with lightweight aggregates. Several process routes, such as partial sintering, in-situ decomposition, adding

pore-forming agent, direct foaming, and superplastic foaming, have been developed to fabricate lightweight aggregates. The pore structure characteristics are primarily responsible for the properties of lightweight aggregates and the corresponding lightweight refractories. In general, lightweight aggregates with a high proportion of closed porosity and small pore size are desirable.

The properties of a lightweight refractory are affected by many internal and external factors. Besides the phase composition and microstructure of lightweight aggregates, the particle packing of the matrix and density gradient of the refractory are also of significant importance. Moreover, the service conditions, such as slag compositions, atmospheric conditions, and external field, should be considered during the service of lightweight refractories. After approximately 20 years of rapid development, optimising the compositions, structural characteristics, and service conditions of lightweight refractories has been proved to simultaneously improve energy conservation and life span in certain industrial or laboratory experiments.

After a systematic overview of the processing and application of lightweight wear lining refractories, we opine that the following topics should be considered in future studies.

(i) New process routes should be developed for lightweight aggregates. The properties of lightweight aggregates depend primarily on their pore structure characteristics. Requirements on the pore structure characteristics could be different for various service conditions. Thus, the pore structure characteristics should be regulated or even customized, which is difficult to achieve considering the existing processing routes. The regulations could be adapted from other fields, such as additive manufacturing techniques (3D printing) or novel core-shell structures. We hope that new advanced processing routes are developed in the future.

(ii) Intrinsic mechanism of the service performance and degradation behaviour of

lightweight refractories. When compared to conventional dense refractories, further contributing factors influence the performance of lightweight refractories. Owing to the influence of porosity, the bonding degree, mechanical behaviour, and degradation mechanism of two refractories are very different. Further attention should be focused on the service and degradation behaviour of lightweight refractories. In particular, it is an urgent requirement to understand the correlations of each influential factors on the performance of lightweight refractories, which may provide guidelines pertaining to the fabrication of lightweight aggregates.

(iii) Integrated design of refractory linings for industrial furnaces. With the application of lightweight wear lining refractories, the temperature distribution fields of furnace linings change significantly, and consequently, the requirements for the safety lining and insulation layer also change. Studies have thus far focused only on the performance of lightweight wear linings, while the collocation of safety linings and insulation layers has drawn little attention. More studies should consider the integrated design of refractory linings to exploit the advantages of lightweight wear linings.

Acknowledgements

This work is financially supported by the National Natural Science Foundation of China (Grant Nos. 51802231, 52172023, and 51474165), the Hong Kong Scholars Program 2020 (Grant No. G-YZ4E/ XJ2020023), the China Postdoctoral Science Foundation (Grant Nos. 2018T110811 and 2017M622535) and the WUST National Defence Pre-research Foundation (Grant No. GF201905).

References

[1] A.M. Paramonov, Heating furnaces efficiency improvement, Procedia. Eng. 113 (2015)

181–185. https://doi.org/10.1016/j.proeng.2015.07.315

[2] Ü. Çamdali, M. Tunç, Steady state heat transfer of ladle furnace during steel production process, J. Iron. Steel. Res. Int. 13 (2006) 18-20. https://doi.org/10.1016/S1006-706X(06)60054-X

[3] R. Sarkar, S. Sengupta, Gradient refractories: a new concept for refractory linings, Int. Ceram. Rev. 68 (2019) 28–33. https://doi.org/10.1007/s42411-019-0038-3

[4] A. Huang, H. Harmuth, M. Doletschek, S. Vollmann, X.Z. Feng, Toward CFD modeling of slag entrainment in gas stirred ladles, Steel. Res. Int. 85 (2015) 1447-1454. https://doi.org/10.1002/srin.201400373

[5] Y.S. Zou, A. Huang, L.P. Fu, P.F. Lian, Y.J. Wang, H.Z. Gu, Chemical interactions between a calcium aluminate glaze and molten stainless steel containing alumina inclusions, Ceram. Int. 44 (2018) 1099–1103. https://doi.org/10.1016/j.ceramint.2017.10.057

[6] Y.S. Zou, A. Huang, H.Z. Gu, Novel phenomenon of quasi-volcanic corrosion on the alumina refractory-slag-air interface, J. Am. Ceram. Soc. 103 (2020) 6639–6649. https://doi.org/10.1111/jace.17394

[7] L.G. Chen, A. Malfliet, J. Vleugels, B. Blanpain, M.X. Guo, Degradation mechanisms of alumina-chromia refractories for secondary copper smelter linings, Corros. Sci. 136 (2018) 409–417. https://doi.org/10.1016/j.corsci.2018.03.039

[8] J.F. Chen, J.L. Xiao, Y. Zhang, Y.W. Wei, Y.Q. Li, S.W. Zhang, N. Li, Degradation mechanism of Cr_2O_3-Al_2O_3-ZrO_2 refractories in a coal-water slurry gasifier: Role of stress cracks, J. Am. Ceram. Soc. 103 (2020) 3299–3310. https://doi.org/10.1111/jace.17001

[9] M.H. Wu, A. Huang, S. Yang, H.Z. Gu, L.P. Fu, G.Q. Li, H.Y. Dong, Corrosion mechanism of Al_2O_3–SiC–C refractory by SiO_2–MgO-based slag, Ceram. Int. 46 (2020) 28262–28267. https://doi.org/10.1016/j.ceramint.2020.07.327

[10] S. Ng, B.P. Jelle, L.I. Sandberg, T. Gao, S.A. Mofid, Hollow silica nanospheres as thermal insulation materials for construction: Impact of their morphologies as a function of synthesis pathways and starting materials, Constr. Build. Mater. 166 (2018) 72-80. https://doi.org/10.1016/j.conbuildmat.2018.01.054

[11] K. Lin, Z.J. Shen, Q.F. Liang, J.L. Xu, H.F. Liu, Modelling study of characteristics of heat transfer and structural optimization of refractory layer in an entrained-flow gasifier, Appl. Therm. Eng. 168 (2020) 114830. https://doi.org/10.1016/j.applthermaleng.2019.114830

[12] K.D. Peaslee, S.N. Lekakh, J.D. Smith, M. Vibhandik, Increasing energy efficiency through improvements in ladle materials and practices, Proceedings of the Technical and Operating Conference of the Steel Founders' Society of America, Steel Founders' Society of America (SFSA).

[13] R.R. Chen, P.X. He, N. Wang, J.N. Mou, F.F. Gan, Development of a low density castable for steel ladle, Proceedings of the Unified International Technical Conference on Refractories (UNITECR 2003).

[14] S.J. Li, N. Li, Y.W. Li, Processing and microstructure characterization of porous corundum–spinel ceramics prepared by in situ decomposition pore-forming technique, Ceram. Int. 34 (2008) 1241–1246. https://doi.org/10.1016/j.ceramint.2007.03.018

[15] W. Yan, N. Li, Y.Y. Li, G.P. Liu, B.Q. Han, J.L. Xu, Effect of particle size on microstructure and strength of porous spinel ceramics prepared by pore-forming in situ technique, Bull. Mater. Sci. 34 (2011) 1109-1112. https://doi.org/10.1007/s12034-011-0155-8

[16] W. Yan, N. Li, B.Q. Han, J. Liu, G.P. Liu, Preparation and characterization of porous cordierite ceramics with well-distributed interconnected pores, T. Indian. Ceram. Soc. 70 (2011) 65-69. https://doi.org/10.1080/0371750X.2011.10600150

[17] W. Yan, H. Luo, J. Tong, N. Li, Effects of sintering temperature on pore characterization

and strength of porous cordierite–mullite ceramics by a pore-forming in-situ technique, Int. J. Mater. Res. 103 (2012) 1239-1243. https://doi.org/10.3139/146.110757

[18] W. Yan, N. Li, B.Q. Han, Preparation and characterization of porous ceramics prepared by kaolinite gangue and $Al(OH)_3$ with double addition of $MgCO_3$ and $CaCO_3$, Int. J. Min. Met. Mater. 18 (2011) 450-454. https://doi.org/10.1007/s12613-011-0461-6

[19] W. Yan, N. Li, B.Q. Han, Influence of microsilica content on the slag resistance of castables containing porous corundum-spinel aggregates, Int. J. Appl. Ceram. Tec. 5 (2008) 633-640. https://doi.org/10.1111/j.1744-7402.2008.02240.x

[20] R. Salomão, V.L. Ferreira, I.R. Oliveira, A.D.V. Souza, W.R. Correr, Mechanism of pore generation in calcium hexaluminate (CA_6) ceramics formed in situ from calcined alumina and calcium carbonate aggregates, J. Eur. Ceram. Soc. 36 (2016) 4225-4235. https://doi.org/10.1016/j.jeurceramsoc.2016.05.026

[21] C. Wöhrmeyer, J.Y. Gao, C. Parr, M. Szepizdyn, R. Mineau, J.H. Zhu, Corrosion mechanism of a density-reduced steel ladle lining containing porous spinel-calcium aluminate aggregates, Ceramics. 3 (2020) 155-170. https://doi.org/10.3390/ceramics3010015

[22] Z. Chen, W. Yan, S. Schafföner, Y.W. Li, N. Li, Microstructure and mechanical properties of lightweight Al_2O_3-C refractories using different carbon sources, J. Alloy. Compd. 862 (2021) 158036. https://doi.org/10.1016/j.jallcom.2020.158036

[23] L.P. Fu, H.Z. Gu, A. Huang, M.J. Zhang, X.Q. Hong, L.W. Jin, Possible improvements of alumina-magnesia castable by lightweight microporous aggregates, Ceram. Int. 41 (2015) 1263–1270. https://doi.org/10.1016/j.ceramint.2014.09.056

[24] A. Kishimoto, Superplastically foaming method for inclusion of closed pores in fully densified ceramics, J. Ceram. Soc. Jpn. 121 (2013) 527-533. https://doi.org/10.2109/jcersj2.121.527

[25] T. Higashiwada, H. Asaoka, H. Hayashi, A. Kishimoto, Effect of additives on the pore evolution of zirconia based ceramic foams after sintering, J. Eur. Ceram. Soc. 27 (2007) 2217-2222. https://doi.org/10.1016/j.jeurceramsoc.2006.08.008

[26] L.P. Fu, A. Huang, H.Z. Gu, H.W. Ni, Properties and microstructures of lightweight alumina containing different types of nano-alumina, Ceram. Int. 44 (2018) 17885–17894. https://doi.org/10.1016/j.ceramint.2018.06.261

[27] L.P. Fu, A. Huang, H.Z. Gu, H.W. Ni, Fabrication of lightweight alumina containing fine closed pores by controlling the relationship between phase stress and superplasticity: Experimental and mathematical studies, Ceram. Int. 44 (2018) 20034–20042. https://doi.org/10.1016/j.ceramint.2018.07.277

[28] L.P. Fu, H.Z. Gu, M.J. Zhang, A. Huang, C.L. Fan, H.W. Ni, Role of liquid phase amounts in the pore evolution of lightweight bauxite: Experimental and thermal simulation studies, Ceram. Int. 45 (2019) 6216-6222. https://doi.org/10.1016/j.ceramint.2018.12.099

[29] Y.S. Zou, H.Z. Gu, A. Huang, L.P. Fu, G.Q. Li, Fabrication and analysis of lightweight magnesia based aggregates containing nano-sized intracrystalline pores, Mater. Design. 186 (2020) 108326. https://doi.org/10.1016/j.matdes.2019.108326

[30] Y.S. Zou, H.Z. Gu, A. Huang, L.P. Fu, Formation mechanism of in situ intergranular $CaZrO_3$ phases in sintered magnesia refractories, Metall. Mater. Trans. A. 51 (2020) 5328–5338. https://doi.org/10.1007/s11661-020-05919-6

[31] L.P. Fu, H.Z. Gu, A. Huang, Y.S. Zou, H.W. Ni, Enhanced corrosion resistance through the introduction of fine pores: Role of nano-sized intracrystalline pores, Corros. Sci. 161 (2019) 108182. https://doi.org/10.1016/j.corsci.2019.108182

[32] L.P. Fu, A. Huang, P.F. Lian, H.Z. Gu, Isolation or corrosion of microporous alumina in contact with various CaO-Al_2O_3-SiO_2 slags, Corros. Sci. 120 (2017) 211–218.

https://doi.org/10.1016/j.corsci.2017.01.018

[33] L.P. Fu, H.Z. Gu, A. Huang, M.J. Zhang, Z.K. Li, Slag resistance mechanism of lightweight microporous alumina aggregate, J. Am. Ceram. Soc. 98 (5) (2015) 1658-1663. https://doi.org/10.1111/jace.13487

[34] Y. Zou, A. Huang, H.Z. Gu, M.J. Zhang, P.F. Lian, Effects of particle distribution of matrix on microstructure and slag resistance of lightweight Al_2O_3–MgO castables, Ceram. Int. 42 (2016) 1964–1972. https://doi.org/10.1016/j.ceramint.2015.09.167

[35] Y. Zou, H.Z. Gu, A. Huang, M.J. Zhang, C. Ji, Effects of MgO micropowder on microstructure and resistance coefficient of Al_2O_3–MgO castable matrix, Ceram. Int. 40 (2014) 7023–7028. https://doi.org/10.1016/j.ceramint.2013.12.030

[36] Y.L. Xin, H.F. Yin, Y. Tang, Q.F. Wan, K. Gao, H.D. Yuan, Z.W. Wang, Formation mechanism and characterization of gradient density in corundum–spinel refractory, Ceram. Int. 45 (2019) 8023–8026. https://doi.org/10.1016/j.ceramint.2018.12.199

[37] H.F. Yin, Y.L. Xin, J.L. Dang, K. Gao, Y. Tang, H.D. Yuan, Preparation and properties of lightweight corundum-spinel refractory with density gradient, Ceram. Int. 44 (2018) 20478–20483. https://doi.org/10.1016/j.ceramint.2018.08.043

[38] W. Yan, N. Li, B.Q. Han, Effects of sintering temperature on pore characterization and strength of porous corundum-mullite ceramics, J. Ceram. Process. Res. 11 (2010) 388-391.

[39] W. Yan, N. Li, Y.Y. Li, J. Tong, H. Luo, Strength and gas permeability of porous cordierite-mullite ceramics with different phase compositions and microstructures prepared by a pore-forming in-situ technique, J. Ceram. Process. Res. 14 (2013) 109-113.

[40] L.P. Fu, H.Z. Gu, A. Huang, H.W. Ni, Correlations among processing parameters and porosity of a lightweight alumina, Ceram. Int. 44 (2018) 14076–14081. https://doi.org/10.1016/j.ceramint.2018.05.005

[41] R.J. Brook, Pore-grain boundary interactions and grain growth, J. Am. Ceram. Soc. 52 (1969) 56-57. https://doi.org/10.1111/j.1151-2916.1969.tb12664.x

[42] J. Svoboda, H. Riedel, Pore-boundary interactions and evolution equations for the porosity and the grain size during sintering, Acta. Mater. 40 (1992) 2829-2840. https://doi.org/10.1016/0956-7151(92)90448-N

[43] J. Rödel, A.M. Glaeser, Pore drag and pore-boundary separation in alumina, J. Am. Ceram. Soc. 73 (1990) 3302-3312. https://doi.org/10.1111/j.1151-2916.1990.tb06453.x

[44] H.J. Xu, Z.B. Xing, F.Q. Wang, Z.M. Cheng, Review on heat conduction, heat convection, thermal radiation and phase change heat transfer of nanofluids in porous media: Fundamentals and applications, Chem. Eng. Sci. 195 (2019) 462-483. https://doi.org/10.1016/j.ces.2018.09.045

[45] Y. Han, C.W. Li, C. Bian, S.B. Li, C.A. Wang, Porous anorthite ceramics with ultra-low thermal conductivity, J. Eur. Ceram. Soc. 33 (2013) 2573-2578. https://doi.org/10.1016/j.jeurceramsoc.2013.04.006

[46] J. Chen, X.B. Zhang, Pore-size dependence of the heat conduction in porous silicon and phonon spectral energy density analysis, Phys. Lett. A. 384 (2020) 126503. https://doi.org/10.1016/j.physleta.2020.126503

[47] G. Lebon, Heat conduction at micro and nanoscales: A review through the prism of extended irreversible thermodynamics, J. Non-equil. Thermody. 39 (2014) 35-39. https://doi.org/10.1515/jnetdy-2013-0029

[48] M. Kashiwagi, Y. Sudo, T. Shiga, J. Shiomi, Modeling heat conduction in nanoporous silicon with geometry distributions, Phys. Rev. Appl. 10 (2018) 044018. https://doi.org/10.1103/PhysRevApplied.10.044018

[49] G. Pia, L. Casnedi, U. Sanna, Porous ceramic materials by pore-forming agent method:

An intermingled fractal units analysis and procedure to predict thermal conductivity, Ceram. Int. 41 (2015) 6350-6357. https://doi.org/10.1016/j.ceramint.2015.01.069

[50] Z. Živcová, E. Gregorová, W. Pabst, D.S. Smith, A. Michot, Céline. Poulier, Thermal conductivity of porous alumina ceramics prepared using starch as a pore-forming agent, J. Eur. Ceram. Soc. 29 (2009) 347-353. https://doi.org/10.1016/j.jeurceramsoc.2008.06.018

[51] G. Pia, U. Sanna, An intermingled fractal units model to evaluate pore size distribution influence on thermal conductivity values in porous materials, Appl. Therm. Eng. 65 (2014) 330-336. https://doi.org/10.1016/j.applthermaleng.2014.01.037

[52] T. Shimizu, K. Matsuura, H. Furue, K. Matsuzak, Thermal conductivity of high porosity alumina refractory bricks made by a slurry gelation and foaming method, J. Eur. Ceram. Soc. 33 (2013) 3429-3435. https://doi.org/10.1016/j.jeurceramsoc.2013.07.001

[53] H.D. Li, Q. Zeng, S.L. Xu, Effect of pore shape on the thermal conductivity of partially saturated cement-based porous composites, Cem. Concr. Compos. 81 (2017) 87-96. https://doi.org/10.1016/j.cemconcomp.2017.05.002

[54] M.J. Zhang, M.L. He, H.Z. Gu, A. Huang, W.G. Xiang, Influence of pore distribution on the equivalent thermal conductivity of low porosity ceramic closed-cell foams, Ceram. Int. 44 (2018) 19319–19329. https://doi.org/10.1016/j.ceramint.2018.07.160

[55] L.H. He, M.J. Zhang, H.Z. Gu, A. Huang, The influence of thermal radiation on effective thermal conductivity in porous material, Int. Ceram. Rev. 65 (2016) 237–243. https://doi.org/10.1007/BF03401175

[56] W.E. Lee, S. Zhang, Melt corrosion of oxide and oxide–carbon refractories, Int. Mater. Rev. 44 (3) (1999) 77–104. https://doi.org/10.1179/095066099101528234

[57] A.O. Surendranathan. An introduction to ceramics and refractories, CRC Press, Florida, 2015.

[58] C.E. Inglis, Stresses in a plate due to the presence of cracks and sharp corners, Proc. Inst. Nav. Arch., 55 (1913), pp. 219-230

[59] L.J. Vandeperre, J. Wang, W.J. Clegg, Effects of porosity on the measured fracture energy of brittle materials, Philos. Mag. 84 (2004) 3689-3704. https://doi.org/10.1080/14786430412331293522

[60] D. Leguillon, R. Piat, Fracture of porous materials – Influence of the pore size, Eng. Fract. Mech. 75 (2008) 1840-1853. https://doi.org/10.1016/j.engfracmech.2006.12.002

[61] J.F. Yang, T. Ohji, S. Kanzaki, A. Díaz, S. Hampshire, Microstructure and mechanical properties of silicon nitride ceramics with controlled porosity, J. Am. Ceram. Soc. 85 (2002) 1512-1516. https://doi.org/10.1111/j.1151-2916.2002.tb00305.x

[62] Y.J. Luo, H.Z. Gu, M.J. Zhang, A. Huang, H.F. Li, C. Yu, T.S. Li, P.Z. Yan, Research on thermal shock resistance of porous refractory material by strain-life fatigue approach, Ceram. Int. 46 (2020) 14884–14893. https://doi.org/10.1016/j.ceramint.2020.03.015

[63] G. Jean, V. Sciamanna, M. Demuynck, F. Cambier, M. Gonon, Macroporous ceramics: Novel route using partial sintering of alumina-powder agglomerates obtained by spray-drying, Ceram. Int. 40 (2014) 10197–10203. https://doi.org/10.1016/j.ceramint.2014.02.089

[64] T. Ohji, M Fukushima, Macro-porous ceramics: processing and properties, Int. Mater. Rev. 57 (2012) 115-131. https://doi.org/10.1179/1743280411Y.0000000006

[65] L.P. Fu, A. Huang, H.Z. Gu, D.H. Lu, P.F. Lian, Effect of nano-alumina sol on the sintering properties and microstructure of microporous corundum, Mater. Design. 89 (2016) 21-26. https://doi.org/10.1016/j.matdes.2015.09.132

[66] W. Pabst, E. Gregorová, I. Sedlářová, M. Černý, Preparation and characterization of porous alumina–zirconia composite ceramics, J. Eur. Ceram. Soc. 31 (2011) 2721-2731. https://doi.org/10.1016/j.jeurceramsoc.2011.01.011

[67] A. Kocjan, Z.J. Shen, Colloidal processing and partial sintering of high-performance porous zirconia nanoceramics with hierarchical heterogeneities, J. Eur. Ceram. Soc. 33 (2013) 3165-3176. https://doi.org/10.1016/j.jeurceramsoc.2013.06.004

[68] L.P. Fu, H.Z. Gu, A. Huang, Y.S. Zou, M.J. Zhang, Fabrication of lightweight alumina with nanoscale intracrystalline pores, J. Am. Ceram. Soc. 103 (3) (2020) 2262-2271. https://doi.org/10.1111/jace.16914

[69] L.P. Fu, A. Huang, H.Z. Gu, M.J. Zhang, P.F. Lian, Fabrication and characterization of lightweight microporous alumina with guaranteed slag resistance, Ceram. Int. 42 (2016) 8724–8728. https://doi.org/10.1016/j.ceramint.2016.02.107

[70] Y.S. Zou, H.Z. Gu, A. Huang, Y.Z. Huo, L.P. Fu, Y.W. Li, Characterisation and properties of low-conductivity microporous magnesia based aggregates with in-situ intergranular spinel phases, Ceram. Int. 47 (2021) 11063–11071. https://doi.org/10.1016/j.ceramint.2020.12.229

[71] Y.S. Zou, H.Z. Gu, A. Huang, L.P. Fu, G.Q. Li, Fabrication and properties of in situ intergranular $CaZrO_3$ modified microporous magnesia aggregates, Ceram. Int. 46 (2020) 16956–16965. https://doi.org/10.1016/j.ceramint.2020.03.279

[72] L.P. Fu, H.Z. Gu, A. Huang, C. Bai, Effect of MgO micropowder on sintering properties and microstructures of microporous corundum aggregates, Ceram. Int. 41 (2015) 5857–5862. https://doi.org/10.1016/j.ceramint.2015.01.016

[73] Z.Y. Deng, T. Fukasawa, M. Ando, G.J. Zhang, T. Ohji, High-surface-area alumina ceramics fabricated by the decomposition of $Al(OH)_3$, J. Am. Ceram. Soc. 84 (2001) 485-491. https://doi.org/10.1111/j.1151-2916.2001.tb00687.x

[74] Z.Y. Deng, T. Fukasawa, M. Ando, G.J. Zhang, T. Ohji, Microstructure and mechanical properties of porous alumina ceramics fabricated by the decomposition of aluminum hydroxide, J. Am. Ceram. Soc. 84 (2001) 2638-2644.

https://doi.org/10.1111/j.1151-2916.2001.tb01065.x

[75] R. Salomão, M.O.C. V. Bôas, V.C. Pandolfelli, Porous alumina-spinel ceramics for high temperature applications, Ceram. Int. 37 (2011) 1393–1399. https://doi.org/10.1016/j.ceramint.2011.01.012

[76] Y.F. Huang, Z. Chen, W. Yan, Y.J. Dai, G.Q. Li, Q. Wang, N. Li, Y.W. Li, Microstructures and strengths of microporous MgO-Al_2O_3 refractory aggregates using two types of magnesite, Int. J. Appl. Ceram. Tec. 18 (2021) 100-109. https://doi.org/10.1111/ijac.13619

[77] Q.J. Chen, W. Yan, N. Li, X.L. Lin, Z.Y. Zhang, B.Q. Han, Y.W. Wei, Effect of $Al(OH)_3$ content on the microstructure and strength of porous cordierite-mullite ceramics prepared by an in-situ pore forming technique, Sci. Sinter. 50 (2018) 205-215. https://doi.org/10.2298/SOS1802205C

[78] X.L. Lin, W. Yan, N. Li, Phase composition and pore evolution of porous periclase-spinel ceramics prepared from magnesite and $Al(OH)_3$, Sci. Sinter. 48 (2016) 147-155. https://doi.org/ 10.2298/SOS1602147L

[79] W. Yan, Q.J. Chen, X.L. Lin, N. Li, Pore characteristics and phase compositions of porous corundum-mullite ceramics prepared from kaolinite gangue and $Al(OH)_3$ with different amount of $CaCO_3$ addition, J. Ceram. Soc. Jpn. 123 (2015) 897-902. https://doi.org/10.2109/jcersj2.123.897

[80] W. Yan, J.F. Chen, N. Li, B.Q. Han, Y.W. Wei, Lightweight cordierite-mullite refractories with low coefficients of thermal conductivity and high mechanical properties, Bull. Mater. Sci. 38 (2015) 409-415. http://doi.org/ 10.1007/s12034-014-0837-0

[81] W. Yan, J.F. Chen, N. Li, W.D. Qiu, Y.W. Wei, B.Q. Han, Preparation and characterization of porous MgO–Al_2O_3 refractory aggregates using an in-situ decomposition pore-forming technique, Ceram. Int. 41 (2015) 515–520. https://doi.org/10.1016/j.ceramint.2014.08.099

[82] J.N. Zhi, Z. Chen, W. Yan, S. Schafföner, Y.J. Dai, X.L. Lin, Effect of $Al(OH)_3$ particle size on microstructures and strengths of porous $MgAl_2O_4$ ceramics, Process. Appl. Ceram. 14 (2020) 268-275. https://doi.org/10.2298/PAC2003268Z

[83] Z. Miao, N. Li, W. Yan, Effect of sintering temperature on the phase composition and microstructure of anorthite–mullite–corundum porous ceramics, Ceram. Int. 40 (2014) 15795–15799. https://doi.org/10.1016/j.ceramint.2014.07.105

[84] W. Yan, N. Li, J. Tong, G. Liu, J. Xu, Effect of particle size on the pore characterization and strength of porous cordierite-mullite ceramics prepared by a pore-forming in-situ technique, Sci. Sinter. 45 (2013) 165-172. https://doi.org/10.2298/SOS1302165Y

[85] J.T. Qi, W. Yan, Z. Chen, S. Schafföner, W.Y. Zhou, G.Q. Li, Q. Wang, Preparation and characterization of microporous mullite-corundum refractory aggregates with high strength and closed porosity, Ceram. Int. 46 (2020) 8274–8280. https://doi.org/10.1016/j.ceramint.2019.12.056

[86] W. Yan, X.L. Lin, J.F. Chen, N. Li, Y.W. Wei, B.Q. Han, Effect of TiO_2 addition on microstructure and strength of porous spinel ($MgAl_2O_4$) ceramics prepared from magnesite and $Al(OH)_3$, J. Alloy. Compd. 618 (2015) 287–291. https://doi.org/10.1016/j.jallcom.2014.08.169

[87] Z.Y. Zhang, W. Yan, N. Li, S. Schafföner, W.Y. Zhou, Z. Chen, J.W. Wei, Mullite-corundum gas-permeable refractories reinforced by in-situ formed SiC whiskers, Ceram. Int. 46 (2020) 25155–25163. https://doi.org/10.1016/j.ceramint.2020.06.302

[88] W.Y. Zhou, W. Yan, N. Li, Y.B. Li, Y.J. Dai, Z.Y. Zhang, Fabrication and characterization of a mullite-foamed ceramic reinforced by in-situ SiC whiskers, Ceram. Int. 46 (2020) 3132–3138. https://doi.org/10.1016/j.ceramint.2019.10.016

[89] Z. Chen, W. Yan, S. Schafföner, Y.J. Dai, Q. Wang, G.Q. Li, A novel approach to

lightweight alumina-carbon refractories for flow control of molten steel, J. Am. Ceram. Soc. 103 (2020) 4713–4724. https://doi.org/10.1111/jace.17137

[90] H. Nishijima, R. Maki, Y. Suzuki, Microstructural control of porous Al_2TiO_5 by using potato starch as pore-forming agent, J. Ceram. Soc. Jpn. 21 (2013) 730–733. https://doi.org/10.2109/jcersj2.121.730

[91] W. Guo, H.B. Lu, C.X. Feng, J. Sun, H.F. Sun, J. Zhou, J.J. Shen, Low-temperature preparation of porous cordierite-mullite ceramics using rice husk as silica source and pore-forming agent, Appl. Mech. Mater. 217-219 (2012) 86-90. https://doi.org/10.4028/www.scientific.net/AMM.217-219.86

[92] R.P. Liu, C.A. Wang, Effects of mono-dispersed PMMA micro-balls as pore-forming agent on the properties of porous YSZ ceramics, J. Eur. Ceram. Soc. 33 (2013) 1859–1865. https://doi.org/10.1016/j.jeurceramsoc.2013.01.036

[93] Y. Yin, B.Y. Ma, C.B. Hu, G.Q. Liu, H.X. Li, C. Su, X.M. Ren, J.Y. Yu, Y.R. Zhang, J.K. Yu, Preparation and properties of porous SiC–Al_2O_3 ceramics using coal ash, Int. J. Appl. Ceram. Tec. 16 (2019) 25-31. https://doi.org/10.1111/ijac.13080

[94] B. Ren, Y.W. Li, S.B. Sang, S.L. Jin, Lightweight design of bauxite-SiC composite refractories as the lining of rotary cement kiln using alternative fuels, Ceram. Int. 43 (2017) 11048–11057. https://doi.org/10.1016/j.ceramint.2017.05.148

[95] F. Chen, Q. Shen, F.Q. Yan, L.M. Zhang, Pressureless sintering of α-Si_3N_4 porous ceramics using a H_3PO_4 pore-forming agent, J. Am. Ceram. Soc. 90 (2007) 2379–2383. https://doi.org/10.1111/j.1551-2916.2007.01800.x

[96] J.J. Liu, Y.B. Li, Y.W. Li, S.B. Sang, S.J. Li, Effects of pore structure on thermal conductivity and strength of alumina porous ceramics using carbon black as pore-forming agent, Ceram. Int. 42 (2016) 8221-8228. https://doi.org/10.1016/j.ceramint.2016.02.032

[97] J.J. Liu, B. Ren, T.B. Zhu, S. Yan, X.Y. Zhang, W.L. Huo, Y.G. Chen, J.L. Yang, Enhanced mechanical properties and decreased thermal conductivity of porous alumina ceramics by optimizing pore structure, Ceram. Int. 44 (2018) 13240-13246. https://doi.org/10.1016/j.ceramint.2018.04.151

[98] Z.Y. Zhang, W.Y. Zhou, B.Q. Han, Y.B. Li, W. Yan, N.N. Xu, N. Li, J.W. Wei, Preparation and characterization of eco-friendly and low-cost mullite-corundum foamed ceramics with low thermal conductivity, Ceram. Int. 45 (2019) 13203–13209. https://doi.org/10.1016/j.ceramint.2019.04.003

[99] W.Y. Zhou, W. Yan, N. Li, Y.B. Li, Y.J. Dai, B.Q. Han, Y.W. Wei, Preparation and characterization of mullite foam ceramics with porous struts from white clay and industrial alumina, Ceram. Int. 44 (2018) 22950–22956. https://doi.org/10.1016/j.ceramint.2018.09.092

[100] C. Jie, H. Liu, Z.F. Wang, X.T. Wang, Y. Ma, Structure and properties of lightweight magnesia refractory castables with porous matrix, Ceram. Int. 47 (2021) 7880–7887. https://doi.org/10.1016/j.ceramint.2020.11.134

[101] H. Chen, L. Zhao, X. He, W. Fang, Z.X. Lei, H. Chen, The fabrication of porous corundum spheres with core-shell structure for corundum-spinel castables, Mater. Des. 85 (2015) 574–581. https://doi.org/10.1016/j.matdes.2015.07.033

[102] A. Kishimoto, T. Higashiwada, H. Asaoka, H. Hayashi, The exploitation of superplasticity in the successful foaming of ceramics after sintering, Adv. Eng. Mater. 8 (2006) 708-711. https://doi.org/10.1002/adem.200600070

[103] A. Kishimoto, M. Obata, H. Asaoka, H. Hayashi, Fabrication of alumina-based ceramic foams utilizing superplasticity, J. Eur. Ceram. Soc. 27 (2007) 41-45. https://doi.org/10.1016/j.jeurceramsoc.2006.03.002

[104] A. Kishimoto, M. Hanao, H. Hayashi, Improvement in the specific strength by arranging

closed pores in fully densified zirconia ceramics, Adv. Eng. Mater. 11 (2009) 96-100. https://doi.org/10.1002/adem.200800259

[105] S. Hashimoto, T. Umeda, K. Hirao, N. Kondo, Y. Zhou, H. Hyuga, S. Honda, Y. Iwamoto, Fabrication and characterization of porous ZrO_2 with a high volume fraction of fine closed pores, J. Eur. Ceram. Soc. 33 (2013) 61-66. https://doi.org/10.1016/j.jeurceramsoc.2012.08.012

[106] S. Hashimoto, T. Umeda, K. Hirao, N. Kondo, H. Hyuga, Y. Zhou, S. Honda, Y. Iwamoto, Energy efficient synthesis of porous ZrO_2 with fine closed pores by microwave irradiation, Mater. Lett. 93 (2013) 293-296. https://doi.org/10.1016/j.matlet.2012.11.111

[107] M. Obata, H. Hayashi, A. Kishimoto, Alumina-based monofoams utilizing superplastic deformation facilitated by the addition of magnesia or magnesium aluminate spinel, J. Alloy. Compd. 471 (2009) L32–L35. https://doi.org/10.1016/j.jallcom.2008.03.136

[108] L. Yuan, X.D. Zhang, Q. Zhu, G. Wei, J.K. Yu, S.W. Zhang, Preparation and characterisation of closed-pore Al_2O_3-$MgAl_2O_4$ refractory aggregate utilising superplasticity, Adv. Appl. Ceram. 117 (2018) 182-188. https://doi.org/10.1080/17436753.2017.1405555

[109] Z. Chen, W. Yan, Y.J. Dai, S. Schafföner, B.Q. Han, N. Li, Effect of microporous corundum aggregates on microstructure and mechanical properties of lightweight corundum refractories, Ceram. Int. 45 (2019) 8533–8538. https://doi.org/10.1016/j.ceramint.2019.01.168

[110] G.Y. Wu, W. Yan, S. Schafföner, Y.J. Dai, B.Q. Han, T.Q. Li, S.B. Ma, N. Li, G.Q. Li, A comparative study on the microstructures and mechanical properties of a dense and a lightweight magnesia refractories, J. Alloy. Compd. 796 (2019) 131–137. https://doi.org/10.1016/j.jallcom.2019.05.064

[111] W. Yan, X.L. Lin, J.F. Chen, Q.J. Chen, N. Li, Lightweight corundum-mullite refractories: I, Effects of pore characteristics and phase compositions on the slag resistance of

porous corundum-mullite aggregates, J. Ceram. Process. Res. 17 (2016) 161-165.

[112] W. Yan, Q.J. Chen, X.L. Lin, J.F. Chen, N. Li, Lightweight corundum-mullite refractories: II, Effects of porous aggregates on the slag resistances of corundum-mullite refractories, J. Ceram. Process. Res. 17 (2016) 313-317.

[113] R. Sarkar, Particle size distribution for refractory castables: A review, Int. Ceram. Rev. 65 (2016) 82-86. https://doi.org/10.1007/BF03401156

[114] Y. Zou, H.Z. Gu, A. Huang, M.J. Zhang, P.F. Lian, An approach for matrix densification based on particle packing and its effect on lightweight Al_2O_3-MgO castables, Ceram. Int. 42 (2016) 18560–18567. https://doi.org/10.1016/j.ceramint.2016.08.197

[115] H.F. Yin, K. Gao, Q.F. Wan, Y.L. Xin, Y. Tang, H.D. Yuan, A comparative study on the slag resistance of dense corundum-spinel refractory and lightweight corundum-spinel refractory with density gradient, Ceram. Int. in press. https://doi.org/10.1016/j.ceramint.2021.04.138

[116] Y.C. Liu, H.F. Yin, Y. Tang, Y.L. Xin, H.D. Yuan, X.H. Ren, Q.F. Wan, Synthesis mechanism and properties of lightweight mullite-corundum refractories obtained through high temperature liquid-assisted micrometer-scale Kirkendall effect, Ceram. Int. 47 (2021) 9234–9244. https://doi.org/10.1016/j.ceramint.2020.12.049

[117] Q.F. Wan, H.F. Yin, Y. Tang, H.D. Yuan, X.H. Ren, K. Gao, Y.L. Xin, Y.C. Liu, Effect of aggregate on aggregate/spinel matrix bonding interface and mechanical performance of lightweight spinel-bonded refractory, Ceram. Int. 46 (2020) 18362–18365. https://doi.org/10.1016/j.ceramint.2020.04.095

[118] Y.L. Xin, H.F. Yin, Y. Tang, H.D. Yuan, X.H. Ren, K. Gao, Q.F. Wan, Y.C. Liu, Formation mechanism of $MgSrAl_{10}O_{17}$ and its effect on the mechanical performance of lightweight Al_2O_3–$MgAl_2O_4$ refractories, Ceram. Int. 46 (2020) 11075–11079.

https://doi.org/10.1016/j.ceramint.2020.01.127

[119] Q.F. Wan, H.F. Yin, Y. Tang, H.D. Yuan, X.H. Ren, Y.L. Xin, Y.C. Liu, Effect of carbon sources on the properties of lightweight corundum-spinel refractory with density gradient, Int. J. Appl. Ceram. Tec. 17 (2020) 598-605. https://doi.org/10.1111/ijac.13437

[120] Y.L. Xin, H.F. Yin, Y. Tang, H.D. Yuan, X.H. Ren, K. Gao, Q.F. Wan, Y.C. Liu, Effect of alumina bubbles with and without Al_2O_3 coatings on the performance of lightweight Al_2O_3-$MgAl_2O_4$ refractories, Int. J. Appl. Ceram. Tec. 17 (2020) 2622-2628. https://doi.org/10.1111/ijac.13586

[121] M. Maréchal, E.D. C. Estrada, G. Moulin, G. Almeida, L.V. Pin, G. Cuvelier, C. Bonazzi, New insulating and refractory mineral foam: Structure and mechanical properties, Mat. Sci. Eng. A. 780 (2020) 139153. https://doi.org/10.1016/j.msea.2020.139153

[122] T. Juettner, H. Moertel, V. Svinka, R. Svinka, Structure of kaoline–alumina based foam ceramics for high temperature applications, J. Eur. Ceram. Soc. 27 (2007) 1435-1441. https://doi.org/10.1016/j.jeurceramsoc.2006.04.029

[123] J. Stec, J. Tarasiuk, S. Nagy, R. Smulski, J. Gluch, R. Filipek, Non-destructive investigations of pore morphology of micropore carbon materials, Ceram. Int. 45 (2019) 3483-3491. https://doi.org/10.1016/j.ceramint.2018.11.006

[124] W. Yan, N. Li, B.Q. Han, An investigation on slag resistance of castable refractories containing porous spinel aggregates, Int. Ceram. Rev. 58 (2009) 25-29.

[125] W. Yan, J.F. Chen, N. Li, W.D. Qiu, J.H. Ouyang, X.J. He, Influence of light-burned spinel on the slag resistance of alumina-spinel refractory castables, J. Ceram. Process. Res. 15 (2014) 441-446.

[126] X.L. Lin, W. Yan, S.B. Ma, Q.J. Chen, N. Li, B.Q. Han, Y.W. Wei, Corrosion and adherence properties of cement clinker on porous periclase-spinel refractory aggregates with

varying spinel content, Ceram. Int. 43 (2017) 4984–4991. https://doi.org/10.1016/j.ceramint.2017.01.005

[127] G.Y. Wu, W. Yan, S. Schafföner, X.L. Lin, S.B. Ma, Y.J. Zhai, X.J. Liu, L.L. Xu, Effect of magnesium aluminate spinel content of porous aggregates on cement clinker corrosion and adherence properties of lightweight periclase-spinel refractories, Constr. Build. Mater. 185 (2018) 102-109. https://doi.org/10.1016/j.conbuildmat.2018.07.058

[128] Q.J. Chen, W. Yan, N. Li, X.L. Lin, B.Q. Han, Y.W. Wei, Effect of the content of light-burned alumina-spinel composite on the slag resistance of corundum-spinel refractory castables, J. Ceram. Process. Res. 17 (2016) 1100-1105

[129] Z. Chen, W. Yan, S. Schafföner, S.B. Ma, Y.J. Dai, N. Li, Effect of SiC powder content on lightweight corundum-magnesium aluminate spinel castables, J. Alloy. Compd. 764 (2018) 210–215. https://doi.org/10.1016/j.jallcom.2018.06.062

[130] S.B. Ma, W. Yan, S. Schafföner, X.L. Lin, N. Li, Y.J. Zhai, X.J. Liu, L.L. Xu, Influence of magnesium aluminate spinel powder content on cement clinker corrosion and adherence properties of lightweight periclase-spinel refractories, Ceram. Int. 43 (2017) 17026-17031. https://doi.org/10.1016/j.ceramint.2017.09.113

[131] W. Yan, N. Li, B.Q. Han, Effects of microsilica content on microstructure and strength of lightweight castable refractories containing porous corundum-spinel aggregate, Sci. Sinter. 41 (2009) 275-281. https://doi.org/10.2298/SOS0903275Y

[132] H.Z. Gu, A. Huang, Y. Zou, Towards efficient modeling on slag corrosion of lightweight corundum spinel castable for ladle, Proceedings of the Unified International Technical Conference on Refractories (UNITECR 2013). https://doi.org/10.1002/9781118837009.ch147

[133] J.J. Yan, W. Yan, S. Schafföner, Y.J. Dai, Z. Chen, Q. Wang, G.Q. Li, C.J. Jia, Effect of microporous magnesia aggregates on microstructure and properties of periclase-magnesium

aluminate spinel castables, Ceram. Int. 47 (2021) 6540–6547. https://doi.org/10.1016/j.ceramint.2020.10.240

[134] Y. Zou, H.Z. Gu, A. Huang, M.J. Zhang, M.T. Zhang, Effects of aggregate microstructure on slag resistance of lightweight Al_2O_3–MgO castable, Ceram. Int. 43 (2017) 16495–16501. https://doi.org/10.1016/j.ceramint.2017.09.033

[135] P. Yi, P.D. Zhao, D.Q. Zhang, H. Zhang, H.Z. Zhao, Preparation and characterization of mullite microspheres based porous ceramics with enhancement of in-situ mullite whiskers, Ceram. Int. 45 (2019) 14517–14523. https://doi.org/10.1016/j.ceramint.2019.04.161

[136] Z.Y. Zhang, W. Yan, N. Li, Y.B. Li, W.Y. Zhou, B.Q. Han, Influence of spherical porous aggregate content on microstructures and properties of gas-permeable mullite-corundum refractories, Ceram. Int. 45 (2019) 17268–17257. https://doi.org/10.1016/j.ceramint.2019.05.284

[137] M.K. Mahapatra, Review of corrosion of refractory in gaseous environment, Int. J. Appl. Ceram. Technol. 17 (2020) 606-615. https://doi.org/10.1111/ijac.13418

[138] S. Ueno, T. Ohji, H.T. Lin, Corrosion and recession of mullite in water vapor environment, J. Eur. Ceram. Soc. 28 (2008) 431-435. https://doi.org/10.1016/j.jeurceramsoc.2007.03.006

[139] D. Chen, H.Z. Gu, A. Huang, H.W. Ni, Towards chrome-free lining for plasma gasifiers using the CA_6-SiC castable based on high-temperature water vapor corrosion, Ceram. Int. 45 (2019) 12429-12435. https://doi.org/10.1016/j.ceramint.2019.03.175

[140] Y. Zou, H.Z. Gu, A. Huang, Slag corrosion mechanism of lightweight Al_2O_3–MgO castable in different atmospheric conditions, J. Am. Ceram. Soc. 101 (2018) 2096–2106. https://doi.org/10.1111/jace.15337

[141] C.G. Aneziris, M. Hampel, Microstructured and electro-assisted high-temperature

wettability of MgO in contact with a silicate slag-based on fayalite, Int. J. Appl. Ceram. Technol. 5 (2008) 469-479. https://doi.org/10.1111/j.1744-7402.2008.02223.x

[142] Y.S. Zou, A. Huang, P.F. Lian, H.Z. Gu, The interfacial behavior of alumina-magnesia castables and molten slag under an alternating magnetic field, Int. Ceram. Rev. 67 (2018) 36–43. https://doi.org/10.1007/s42411-018-0052-x

[143] A. Huang, P.F. Lian, L.P. Fu, H.Z. Gu, Y.S. Zou, Modeling and experiment of slag corrosion on the lightweight alumina refractory with static magnetic field facing green metallurgy, J. Min. Metall. Sect. B-Metall. 54 (2018) 143–151. https://doi.org/10.2298/JMMB171014002H

[144] Y.S. Zou, A. Huang, R.F. Wang, L.P. Fu, H.Z. Gu, G.Q. Li, Slag corrosion-resistance mechanism of lightweight magnesia-based refractories under a static magnetic field, Corros. Sci. 167 (2020) 108517. https://doi.org/10.1016/j.corsci.2020.108517

[145] C. Tan, Y. Liu, G.Q. Li, C. Yuan, Y.F. Tian, Y.S. Zou, A. Huang, Corrosion behavior of lightweight MgO in high basicity tundish slag, Steel. Res. Int. in press. https://doi.org/10.1002/srin.202100010

[146] G.P. Liu, X.J. Jin, W.D. Qiu, G.Z. Ruan, Y.Y. Li, The impact of bonite aggregate on the properties of lightweight cement-bonded bonite–alumina–spinel refractory castables, Ceram. Int. 42 (2016) 4941–4951. https://doi.org/10.1016/j.ceramint.2015.12.008

[147] W. Yan, G.Y. Wu, S.B. Ma, S. Schafföner, Y.J. Dai, Z. Chen, J.T. Qi, N. Li, Energy efficient lightweight periclase-magnesium alumina spinel castables containing porous aggregates for the working lining of steel ladles, J. Eur. Ceram. Soc. 38 (2018) 4276–4282. https://doi.org/10.1016/j.jeurceramsoc.2018.05.002

[148] W.D. Peng, Z. Chen, W. Yan, S. Schafföner, G.Q. Li, Y.W. Li, C.J. Jia, Advanced lightweight periclase-magnesium aluminate spinel refractories with high mechanical

properties and high corrosion resistance, Constr. Build. Mater. 291 (2021) 123388. https://doi.org/10.1016/j.conbuildmat.2021.123388

[149] T. Hisashi, T. Tomoaki, T. Hidenori, Low thermal conductivity Al_2O_3-MgO-C bricks for steel ladle, Taikabutsu. 62 (2010) 34-35.

[150] P.F. Lian, A. Huang, H.Z. Gu, L.P. Fu, S.S. Wang, Corrosion mechanism of foamed slag on the lightweight corundum-spinel castable, Int. Ceram. Rev. 65 (2016) 226–232. https://doi.org/10.1007/BF03401173

[151] Y.H. Liang, A. Huang, X.W. Zhu, H.Z. Gu. L.P. Fu, Dynamic slag/refractory interaction of lightweight Al_2O_3–MgO castable for refining ladle, Ceram. Int. 41 (2015) 8149–8154. https://doi.org/10.1016/j.ceramint.2015.03.026

[152] H.Z. Gu, L.P. Fu, L.Y. Ma, X. Gao, Y. Zhao, B. Du, Preparation of microporous corundum aggregates and their applications in lightweight alumina-magnesia castables, Int. Ceram. Rev. 63 (2014) 121–124. https://doi.org/10.1007/BF03401045

[153] Y.S. Zou, A. Huang, L.P. Fu, H.Z. Gu, Effect of lightweight refractories on the cleanness of bearing steels, Ceram. Int. 44 (2018) 12965–12942. https://doi.org/10.1016/j.ceramint.2018.04.112

[154] L.P. Fu, Y.S. Zou, A. Huang, H.Z. Gu, H.W. Ni, Corrosion mechanism of lightweight microporous alumina-based refractory by molten steel, J. Am. Ceram. Soc. 102 (6) (2019) 3705-3714. https://doi.org/10.1111/jace.16205